Transient firing of dorsal raphe neurons encodes diverse and specific sensory, motor and reward events

Sachin P. Ranade[1] and Zachary F. Mainen[1,2 *]

[1]Cold Spring Harbor Laboratory
1 Bungtown Road
Cold Spring Harbor, NY 11724

[2]Champalimaud Neuroscience Programme
Instituto Gulbenkian de Ciência
Oeiras, Portugal, P-2781-901

Running Title: Diversity and specificity of raphe transients

* To whom correspondence should be addressed
Phone: +351 214464533
E-mail: zmainen@igc.gulbenkian.pt

ABSTRACT

Serotonin (5-hydroxytryptamine, 5-HT) is known to impact a wide range of behaviors and physiological processes, but relatively little is known about events that trigger 5-HT release. To address this issue, we recorded from neurons in the dorsal raphe nucleus (DRN) in rats performing an odor-guided spatial decision task. A large fraction of DRN neurons showed transient firing time locked to behavioral events on time scales as little as 20 ms. DRN transients were sometimes correlated with reward parameters, but also encoded specific sensorimotor events, including stimulus identity and response direction. These behavioral correlates were diverse but showed no apparent relationship with waveform or other firing properties indicative of neurochemical identity. These results suggest that the 5-HT system does not encode a unitary signal and that it will broadcast specific information to the forebrain with speed and precision sufficient not only to modulate but to dynamically sculpt ongoing information processing.

INTRODUCTION

The 5-HT system is one of the most important targets for treatment of depression, anxiety, panic disorder, chronic pain and other psychiatric conditions. Hence, there has been great interest in elucidating its functions and a large number of pharmacological, as well as genetic, experiments have been performed. These data have implicated 5-HT in modulating an extremely wide range of phenomena, leading to a highly diverse set of behavioral & physiological hypotheses of 5-HT function, including behavioral suppression(Soubrie 1986), defensive behavior(Deakin and Graeff 1991), aversive learning(Daw et al. 2002; Dayan and Huys 2008; Deakin and Graeff 1991), motor facilitation(Jacobs and Fornal 1997), carbon dioxide sensing(Richerson 2004), temporal discounting(Doya 2002) and regulating energy balance(Tecott 2007).

The dorsal raphe nuclei (DRN) are located in the midbrain and control the release of most 5-HT in the neocortex(Jacobs and Azmitia 1992). Electrophysiological recordings of DRN neurons may help to elucidate the function of the 5-HT system by determining the conditions that trigger the firing of these cells and consequent 5-HT release. The first recordings in anaesthetized animals revealed a strong correlation with behavioral state, with DRN firing being minimal during REM sleep and maximal during waking(McGinty and Harper 1976; Trulson and Jacobs 1979). While these remain the most widely documented correlates of DRN firing(Urbain et al. 2006), many physiological variables are also correlated with arousal state, and might account for the observed relationships. Moreover, an extensive series of studies in awake cats found that

the firing rates of putative 5-HT neurons are unaffected by a host of manipulations that would be expected to engage various physiological and behavioral responses, including theromoregulatory, cardiovascular and glucoregulatory challenges, as well as stress from white noise, restraint or predator exposure, and treadmill locomotion(Jacobs and Fornal 1997; Veasey et al. 1997)

Whereas these studies primarily focused on longer time scale DRN modulation, consistent with the classical view of neuromodulatory systems as tonically acting signals, relatively less attention has been focused on transients. If 5-HT neurons signal specific behavioral or cognitive variables(Cools et al. 2008), as has been proposed for the dopamine and norepinephrine systems(Aston-Jones and Cohen 2005; Schultz et al. 1997), then transient signals should be particularly revealing(Schultz 2007). It was observed in early studies that DRN neurons respond rapidly and transiently to peripheral nerve stimulation(Aghajanian et al. 1978), consistent with an aversive signal. A recent study in primates(Nakamura et al. 2008), using a decision-making task, demonstrated DRN neuron firing is modulated both positively and negatively by predicted and received reward magnitude. These results support the involvement of 5-HT in reward processing, but did not reveal a unitary signal as observed for DA neurons(Schultz 2007). They also demonstrate the importance of appropriate behavioral paradigms to rigorously test neuronal correlates.

Transient responses of DRN neurons to sensory stimuli including flashes, sound clicks and light touch(Fornal et al. 1996; Heym et al. 1982; Montagne-Clavel et al. 1995;

Waterhouse et al. 2004), as well as relatively specific motor-related responses(Kulichenko and Pavlenko 2004; Veasey et al. 1995) have been reported, suggesting that even the association of DRN transients and reward is narrow. However, the nature of transient DRN sensory and motor responses has not been extensively documented, particularly since the low firing rates of neurons requires a structured behavioral paradigm to characterize. Therefore, in the present study, we recorded DRN activity in freely moving rats performing a decision-making task.

The use of a two-alternative choice discrimination paradigm provided sensory, motor and reward components and allowed us to correlate neuronal activity across a large number of repeated trials with a variety of behavioral variables with precise timing. We report that a large majority of DRN neurons are rapidly and transiently modulated by sensory and motor as well as reward variables. These responses were more diverse and selective than has previously been appreciated, particularly for sensory and motor variables. These results demonstrate that the DRN processes a wide range of information and suggest that transient 5-HT signals from the DRN will broadcast surprisingly detailed information to the neocortex.

MATERIALS AND METHODS

Animal subjects

Male Long Evans rats weighing 250-350 g were used for all experiments. Rats had free access to food but water was restricted to behavioral session and approximately 30 additional minutes in their home cage such that weights were maintained within 85% of their free feeding weight. All procedures involving animals were carried out in accordance with National Institutes of Health standards as approved by the Cold Spring Harbor Laboratory Institutional Animal Care and Use Committee.

Two-odor discrimination task

All behavioral procedures were conducted as previously described in Uchida and Mainen (2003). Briefly, behavioral setup consisted of a box with a panel containing three ports equipped with infrared photodiode and phototransistor. Interruption of the infra-red photo beam signaled time of entry of rat into the port. Odors were mixed with pure air to produce a 1:10 dilution at a flow rate of 1 l/min using a custom-built olfactometer. Delivery of odors and water reinforcement were controlled using computer data acquisition hardware (National Instruments, Austin, TX, USA) and custom software written in MATLAB.

Rats were trained and tested on a two-alternative choice odor discrimination task as follows. Rats initiated a trial by poking their nose into the central odor-sampling port, which triggered delivery of one of two odors after a random delay of 0.3–0.5 s. After waiting at the odor sampling port for a period of at least 0.1 s, the rat was free to respond by withdrawing from the odor port and moving to the left or right choice ports. Each odor signaled availability of water in one of the two choice ports. Odors used were 1/10 dilutions of (+)- and (-)-enantiomers of 2-octanol in mineral oil. Odor–choice port associations were held constant for all sessions. For 3 rats, pure odor dilutions were used, while for the remaining 4 rats a 95:5 ratio mixture was used.

Upon entry into the correct choice port, water was delivered after a delay according to one of 3 schedules:

(a) fixed delay of 1 s (n = 16 neurons);

(b) fixed delay of 1 s with probability of 0.9 and 2 s with probability 0.1 (n = 21 neurons);

(c) exponential distribution with a mean of 0.8s (n = 4 neurons).

Reward volume for a correct response was 20-25 µl and was calibrated regularly to ensure equal delivery at both ports.

Rats were well trained on the task and reliably completed around 200-300 trials in sessions of 45-120 minutes before micro-drive implantation. Behavioral sessions from the recordings reported in this study had a median of 190 trials (minimum 30 and

maximum 706 trials). Although the median inter trial interval was 10 s, subjects paused occasionally to rest and on several occasions (n = 31 neurons) entered sleep (measured by hippocampal EEG; see Fig. 1E).

Surgical procedures

Rats were anesthetized with a solution of ketamine and medetomidine and mounted in a stereotax. The skull surface was prepared for surgery and an approximately 2-3 mm diameter hole was drilled above the DRN. All co-ordinates were relative to bregma (-7.4 AP, 0.0 L, 6 DV). The underlying sinus was punctured using a fine needle and ensuing bleeding was controlled with gel foam soaked in ACSF. An 18.5 gauge stainless steel guide cannula was inserted through the sinus up to a depth of 3 mm from skull surface and fixed to the skull using dental acrylic. The dummy cannula was slowly removed after 30 – 45 minutes and the guide tube of the tetrode micro-drive was inserted through the cannula. A bipolar electrode was positioned over the hippocampus (-3.0 AP, 2.0 L, 3.2 DV). Cortical EEG was recorded with a stainless steel screw over the cortex (+4.0 AP, -1.0 L). Animal was administered analgesic Ketofen and allowed a week for recovery before commencing water deprivation.

Tetrode recordings

All recording procedures were as previously described (Feierstein et al. 2006). Briefly, recordings were performed using a custom-built micro-drive with 3-5 movable (either individually or in a bundle) tetrodes. Tetrodes consisted of four twisted 17 µm platinum–

iridium wires (Neuralynx, Tuscon, AZ, USA). Tetrodes were advanced slowly through steps of 40 µm and the DRN was defined as the area following a region of low electrical noise as the tetrodes passed through the ventricle. Electrode tracks were visualized by coating a fluorescent marker, DiI (Molecular Probes, Eugene, OR, USA) near the tip of the tetrode. The final position of each track was marked by making an electrical lesion (Fig. 1C).

Analysis

CV2: Variability of spike train was measured using a metric CV2. CV2 is a measure of spike train variability that is not sensitive to mean firing rate as well as slow changes in firing rate. CV2 is a measure of variability of adjacent inter-spike-intervals (ISI). It is the average measure of the variance of 2 adjacent ISIs. CV2 is lower for regular spike trains and higher for irregular spike trains.

Definition of behavioral epochs: The task engaged state (T) was the time spent by rat performing the task. It was defined as the time interval containing at least one port entry every 2 s. The sleep state (S) was defined from hippocampal LFP and the cortical EEG as follows. Sleep bouts were identified by increased power in lower frequency (delta-theta band) and decrease in power in the gamma band (Fig. 1E). The awake state (A) was defined as the time when the rat was neither sleeping nor performing the task. The task modulation index (MI_T) was calculated as the ratio of difference in firing rate between task-engaged and awake state to the sum of the firing rates during the two

epochs $MI_T = \frac{f_T - f_A}{f_T + f_A}$. A sleep modulation index (MI_S) was calculated similarly. The modulation indices have a range between -1 and 1, with 0 indicating no change, negative values indicating suppression of firing with respect to awake firing rate, and positive values indicating enhancement.

Receiver operator characteristic analysis (ROC): ROC was used as a measure of modulation of firing rates within fixed windows during the task. ROC analysis originates from signal detection theory(Green and Swets 1966) and measures the ability of an ideal observer to assign on a trial by trial basis a signal to two distributions. For distributions A and B, the area under the ROC curve $ROC_{area}(A,B)$, ranges from 0 (when values of A are all larger than any value of B) to 1 (when the opposite holds), with 0.5 indicating indistinguishable distributions. Non-parametric ROC analysis does not require assumptions of normality of underlying distributions. ROC based measures have been extensively used for comparing neuronal responses to stimuli and to provide a quantitative estimate of how well the neuronal response is able to classify the stimulus (Britten et al. 1992). A detailed explanation of ROC analysis is described elsewhere(Feierstein et al. 2006). Time windows (epoch) for analysis of firing rates were aligned with respect to specific behavioral events. Fig. 2B shows all epoch windows used in the analysis. Trials where a second behavioral event occurred within the analysis window were excluded. An optimal window size of 300 ms was determined to enable inclusion of maximum number of trials. Only units with at least 10 trials per condition were included. Statistical significance of ROC values was determined using a

permutation test: We recalculated ROC values after randomly reassigning all firing rates to either of the two groups arbitrarily, repeated this procedure 1000 times to obtain a distribution of ROC values, and calculated the fraction of random values exceeding the actual ROC value. For all analyses, we tested for significance at $P = 0.01$.

ROC modulation index (RMI): To compare firing rate modulation during a behavioral epoch with respect to baseline firing rate, we defined an ROC modulation index, $RMI_E = 2 \cdot \left(ROC_{AREA}(f_E, f_B) - 0.5 \right)$, where f_E is the distribution of firing rates across trials for epoch E and f_B is the distribution of firing rates across trials for the baseline epoch. Thus, if distribution of firing rates during an epoch was lower than baseline, RMI has negative values (suppression) while an increase in firing rate generates positive RMI values (enhancement). The baseline distribution was formed by randomly selecting n time intervals of 300 ms from periods during the awake (non-task) state, where n was chosen to match the number of trials contributing to the behavioral epoch firing rate distribution.

Preference index: To compare two trial conditions within the same epoch, we defined a *preference* index as in Feierstein et al. (2006), $PREF_{A,B} = 2 \cdot \left(ROC_{AREA}(f_A, f_B) - 0.5 \right)$, where f_A and f_B are the firing rate distributions for trials of each of two conditions (e.g. odors or movement directions). For this index, +1 indicates preference for one odor or movement condition while -1 indicates opposite preference.

Peri-stimulus time histograms (PSTH) were binned with a time window of 15 ms and smoothed with a Gaussian filter of standard deviation 30 ms.

Z-score: For sliding z-score analysis shown in Fig. 7B, each time bin in the smooth PSTH was transformed to a z-score by subtracting from it the mean and dividing by the standard deviation for entire PSTH for the neuron. Neurons were sorted by their average z-score value during the odor sampling period for plotting in Fig. 7B.

RESULTS

We recorded the activity of 52 neurons in the DRN of seven freely-behaving rats. Recording electrodes (tetrodes) were targeted to DRN using a guide cannula(Waterhouse et al. 2004) to obtain access through the midline sinus (Fig. 1a; see Experimental Procedures). Electrode tracks were recovered using standard histological methods at the termination of the experiment (Fig. 1c). In the subsequent analyses, all neurons recorded within the anatomical boundaries of the DRN (Fig. 1a,b, shaded area) were included.

Firing properties of DRN neurons are heterogeneous

Previous recording studies have identified putative 5-HT neurons on the basis of a wide action potential waveform and metronomic, low frequency firing(Aghajanian and Vandermaelen 1982; Trulson and Jacobs 1979). However, recent studies indicate that this is neither a necessary nor a sufficient criterion(Allers and Sharp 2003; Hajos et al. 2007; Urbain et al. 2006). In our study, DRN neurons showed heterogeneous extracellular waveforms (Fig. 1d). We classified DRN units with spike width greater than 1.2 ms as wide spiking (WS) and the remainder as narrow spiking (NS) (Fig. 1d, Supplementary Fig. 1a, WS: orange; NS: blue). Average firing rates of DRN neurons ranged from 0.01 to 28 spikes/s with a mean of 3.3 spikes/s and showed wide range of firing regularity, as measured by CV2 (see Experimental Procedures), ranging from 0.25 to 1.40 with a mean

of 0.85. Neither mean firing rate nor firing variability correlated with spike width (Supplementary Fig. 1b,c).

A hallmark of putative 5-HT neurons from classical electrophysiological recordings is slow, tonic modulation of firing rate across the sleep-wake-arousal cycle(Trulson and Jacobs 1979). We examined firing rates of DRN neurons during three behavioral states: sleep, task-engaged, and awake but not task-engaged. These states were identified by analyzing behavioral activity and hippocampal LFP (Fig. 1e,f; see Experimental Procedures). The strength of state-dependent modulation was quantified by calculating a normalized index of the change in average firing rate relative to the awake, non-task engaged state (see Experimental procedures). DRN neurons showed a range of sleep and task modulation, with an overall trend for suppression of firing rate during sleep (Fig. 1g; mean sleep index = 0.81 ± 0.32) and enhancement of firing rate in the task-engaged state (Fig. 1h; mean task index = 1.24 ± 0.58). There was no significant correlation between spike width and sleep modulation (Fig. 1g; R^2 = 0.002, N.S.) or task modulation (Fig. 1h; R^2 = 0.014, N.S). We also examined the relationship between other firing properties, namely firing rate and CV2, with state-dependent rate modulation. There was no significant correlation between firing rate of the neuron and degree of state-dependent modulation (R^2 = 0.0003, N.S. for sleep index and R^2 = 0.006, N.S. for task index, Supplementary Fig. 2a,c). There was no correlation between the variability of inter spike interval as measured by CV2 and sleep index (R^2 = 0.037, N.S., Supplementary Fig. 2b), but there was a significant positive correlation with task index (R^2 = 0.162, $p < 0.01$,

Supplementary Fig. 2d). Thus, task-modulated neurons tend to be more bursty than average.

DRN neurons exhibit diverse firing patterns time-locked to task events

In order to examine how DRN neurons respond to behavioral events, we correlated neuronal firing with events during the performance of a two-alternative choice odor discrimination task(Uchida and Mainen 2003). In this task, the rat sampled the odor stimulus at the center port and responded by moving to one of two choice ports located on either side where water was delivered for correct responses. The timing of entry into and exit from the three ports (center odor port, and left and right water ports) was monitored using infrared phototransistor/LED pairs, enabling us to correlate DRN firing with locomotor activity in relationship to port entry and exits. In addition, the timing of odor and water delivery was controlled by computer-actuated solenoid valves, enabling us to correlate DRN firing with stimulus and reward delivery (Fig. 2a).

Most DRN neurons responded during the task with changes in firing rate. Rats performed 255 ± 190 trials per session, allowing us to detect firing rate modulation even in neurons with low firing rates. Fig. 2b shows normalized peri-stimulus time histograms as pseudocolor maps for all recorded neurons time locked to all six behavioral events. DRN neurons show a diverse set of responses, encompassing a range of patterns. Many DRN responses were very transient and tightly locked to specific task events (e.g. Fig.

2b; neurons 23, 30). To quantify these patterns of firing rate modulation, we compared the firing rates in different behavioral epochs (defined as 300 ms fixed time windows relative to specific behavioral events, Fig. 2b, bottom) to the baseline firing rate using a receiver operator characteristic (ROC)-based metric that we refer to as the ROC modulation index (RMI). RMI ranges from -1 to 1, with negative values denoting suppression of firing and positive values enhancement (see Experimental Procedures). Eleven of 52 neurons were excluded from these analyses due to very low firing rates during the task (e.g. Fig. 2b, neuron numbers indicated in red).

As a population, approximately equal numbers of DRN neurons responded during each different epoch of a behavioral trial. Modulation during most epochs was characterized by increase in firing rate, with the exception of the reward epoch where approximately half of the modulated neurons were suppressed (Fig. 2c). Most neurons responded to two or more events (Fig. 2d, e.g. Fig. 2b: 16, 37) although some responded to only one (e.g. Fig. 2b: 9, 30) while a small fraction of neurons appeared to be completely insensitive to task events showing extremely steady, clock-like firing (around 10%, 4 of 41; e.g. Fig. 2b: 5, 47). There was no apparent correlation between the extent of state dependent modulation and strength of transient modulation (R^2 = 0.004, N.S., Fig. 2e). Furthermore, neither spike width (R^2 = 0.055, N.S., Fig. 2f) nor interspike interval variability (R^2 = 0.036, N.S., Supplementary Fig. 3b) showed any correlation with the strength of transient modulation, as will be discussed further below. There was a weak but significant positive correlation between firing rate and strength of modulation (R^2 = 0.25; $p < 0.01$, Supplementary Fig. 3a). Thus, DRN neurons showed a high degree

of heterogeneity of firing properties and exhibited substantial transient modulation time-locked to behavioral events. In the next sections, we will examine in detail the behavioral correlates of raphe neurons during the different phases of the task.

Locomotor correlates of DRN firing are context-dependent

A large fraction of neurons (83%; 34 of 41) showed significant firing rate modulation (measured using RMI, at a criterion of $p < 0.01$, see Experimental Procedures) during either entry or exit from the odor and/or choice ports. In order to determine whether these responses were more closely related to general movement/locomotion or alternatively if they might reflect other abstract variables, we compared the responses of neurons during approach to and withdrawal from the ports. Approach and withdrawal both involve motor "activation" but differ in the specific muscle groups involved as well as the context and goal of the action. Of the 34 modulated neurons, ten (29%) neurons had similar modulation at both ports (i.e. odor or choice) and entry or exit, suggesting a general locomotor correlate (Fig. 3a). Most of these neurons also responded to other task events; for e.g. Neuron in Fig. 3a also shows click-evoked response (discussed later). The remaining two-thirds of neurons (71%, 24 of 34; RMI at $p < 0.01$) were modulated selectively during specific actions (i.e. entry or exit), at specific ports or a combination of both. Fig. 3c shows example of a neuron that fired only in response to exit from the choice ports but not from the odor port. A particularly prominent type of selective modulation was an increase in firing as the animal approached the odor port to initiate the

trial (43%, 18 of 42; RMI at $p < 0.01$). While a majority of these neurons also responded during water port entry, a few neurons (22%, 4 of 18; RMI at $p < 0.01$) showed a ramp in firing exclusively during odor port entry (Fig. 3b). The proportions of neurons with selective locomotor correlates are summarized separately for port approach (Table 1a) and port withdrawal (Table 1b).

In addition to locomotion, the task sequence also involved periods of motor suppression when the rat held its snout in either the odor port awaiting the odor stimulus or the water port awaiting water delivery. Although the mechanics of movement inhibition was very similar at the two types of ports, inhibition of firing was often restricted to only the odor port (43%, 3 of 7 neurons; Fig. 3d) or water port (50%, 4 of 8 neurons). Thus, suppression of firing during nose pokes also appeared to be specifically related to task requirement rather than to holding, waiting or movement cessation per se. The specificity of responses suggests that DRN neurons do not simply respond to gross motor components of the task but instead or in addition to the context in which those movements are executed.

DRN neurons tuned to specific odor stimuli and movement directions

The above analysis points toward substantial specificity of DRN responses. To further this analysis, we examined firing in relation to specific trial types. That is, during each trial one of two different odors is presented and is rewarded for selection of one of two

choice ports, yielding four trial types (two stimuli times two responses). Several DRN neurons preferentially responded to presentation of one of the two odor stimuli (Fig. 4a). We quantified this tuning specificity by defining a *preference* metric scaled between -1 and 1, where 0 indicates no difference in firing rate for the two odors, negative values indicate preference for odor A (S(+)-Octanol) and positive values indicate preference for odor B (R(-)-Octanol)(Feierstein et al. 2006). Of the 28 neurons that showed significant RMI during odor sampling, ten neurons showed significant *preference* values ($p < 0.01$, using a permutation procedure, see Experimental Procedures) during the odor sampling period indicative of odor selective firing (Fig. 4c).

During each trial the rat responded by movement to either the left or right choice port to obtain water. Of the 31 neurons that showed significant modulation during movement to the choice port, nine (29%) were selective (by calculation of *preference* at $p < 0.01$) for one of the two directions of movement (Fig. 4b,d). These results demonstrate a strong specificity of tuning of DRN neurons to alternative stimuli or actions. Only two of 17 odor or direction selective neurons maintained selectivity during both epochs.

Prominence of transient responses to solenoid valve click

A large fraction of DRN neurons showed firing rate modulation during the reward phase of the task (Fig. 2c). The predominant modulation during this behavioral epoch was a transient response triggered by the solenoid valve that was activated to deliver water (Fig.

5a). Around half of the neurons recorded with the solenoid click (43%, 10/23 neurons), showed a significant click-evoked response (RMI at $p < 0.01$). These responses were rapid, with latencies as low as 20 ms, and transient, with duration typically less than 200 ms (Fig. 5a-c, Supplementary Fig. 4a). In some cases, the response consisted of a single spike without apparent change in the overall firing rate (Fig. 5a, Supplementary Fig. 4b). In order to further characterize the properties of these click-responsive neurons, in a subset of sessions ($n = 18$ neurons), we silenced the solenoid valve by placing it outside the recording chamber and substituted it by a pure tone (8 kHz) delivered coincident with water port entry. The pure tone predicted water as faithfully as the click of the valve but was different in its acoustic properties, being narrow band as opposed to the broadband click stimulus which had a higher initial sound intensity. Moreover, during initial stages of training, rats often showed a startle response to the sound of the water valve, but they never did so in response to the tone. On the other hand, 2/18 neurons tested with pure tone showed a significant phasic tone-evoked response (RMI at $p < 0.01$). The relative proportions of click versus tone responsive neurons is significantly different (two-tailed Fischer's exact test, $p < 0.05$), peak latencies of tone responses were relatively long and absolute changes in firing rates for click response were significantly higher than those for tone responses (Mann-Whitney U test $p<0.01$; Fig. 5b).

Reward timing is reflected in DRN firing

Delivery of water was delayed by several different schedules across different recording sessions (see Experimental Procedures). The delay schedules included both fixed (1 s) and random (exponential with mean of 0.82 s) distributions and helped to facilitate identification of reward responses and to allow us to check for relationship of firing to reward timing. In addition, water was omitted on a small subset (20%) of correct responses, a manipulation that can be considered a mildly aversive event. Rats showed no overt response to reward omissions, but left the choice port sooner than when water was delivered. This procedure allowed us to look for correlates of reward anticipation (timing prediction) as well as omission.

In a small subset of neurons, the time course of modulation of firing rate coincided very well with the average delay to the onset of water delivery. Fig. 6a shows a neuron that showed decrease in firing rate that accumulated until the time of expected reward. Similar behavior was observed in four neurons. In order to test for correlates of reward omission, we compared firing rate distributions in correct trials where water was delivered with trials where water was omitted using a sliding ROC analysis (see Experimental Procedures). Note that fewer neurons were eligible for this analysis because we required a minimum number of 10 correct reward-omitted trials. Interestingly, a small subset of neurons (12% or 4/32; *Preference* at $p < 0.01$) responded with a change in firing rate during omission trials around the expected time of reward (Fig. 6b,c and Supplementary Fig. 5a,b). It is important to note that no overt sensory signal occurs at the

time of reward omission and they are in this sense indicative or predictive or internally-generated activity. Also note that the omission responses are correlated with differences in movement that occur not during but subsequent to reward omission.

As noted earlier (Fig. 2d), many neurons responded during more than two epochs within the task. Our dataset did not allow for quantitative analysis of all combinations of observed responses; however one response profile was particularly prominent. A large proportion of click-responsive neurons also exhibited suppression of firing during odor sampling and an increase in firing during movement to water port (Fig. 7a,b). Conversely, neurons that were inhibited while waiting at the water port were often excited during odor sampling (Fig. 7b).

DRN behavioral correlates do not correlate with waveform properties

We have shown that rat DRN neurons respond to diverse sensory, motor and reward-related events. We examined whether the task-related responses showed any correlation with spike characteristics indicative of 5-HTergic and non-5-HTergic neurons. Neither spike width (Fig. 8) nor firing rate and firing variability (Supplementary Fig. 6) were correlated with firing rate modulation during any of the task epochs. Furthermore, the response characteristics of the best candidate "classical" 5-HT neurons (wide spike, low firing rate, sleep suppression) spanned the entire range of observed behavioral correlates, including odor selectivity, valve click response (Fig. 5a), odor port specific inhibition,

reward timing and reward omission. Thus, we found no evidence that putative 5-HTergic neurons or non-5-HTergic DRN neurons display a special class of behavioral correlates.

DISCUSSION

We recorded from the DRN in rats performing a decision-making task. The large majority (70%) of DRN neurons was rapidly modulated by behavioral events on time scales of 200 ms and as little as 20 ms. DRN firing was highly heterogeneous and correlated with a diverse range of sensory and motor events spanning all major elements of the task. Most DRN neurons were activated by more than one type of event but often displayed a surprising degree of stimulus or motor specificity. However, there was no relationship between the behavioral correlates of a particular unit and any physiological criteria (e.g. spike width) traditionally used to classify putative 5-HT neurons.

It has commonly been assumed that the signal carried by a central neuromodulator is a unitary one. In contrast, we observed a striking diversity of behavioral correlates across a population of DRN neurons. Two potential bases for this diversity are the diversity of cell types within the DRN and the anatomical diversity of its connectivity. Neurochemically, an estimated 30-50% neurons in the rat DRN contain 5-HT(Descarries et al. 1982), while a variety of other transmitters are expressed by non-5-HT DRN neurons or co-expressed by 5-HT neurons(Jacobs and Azmitia 1992; Lowry et al. 2008; Michelsen et al. 2007). DRN recordings performed without pre-selection have presented greater diversity of firing profiles, e.g. sleep state modulation(Urbain et al. 2006), than those using traditional criteria. Recent studies show that the criteria used in extracellular recordings are neither necessary nor sufficient to positively identify 5-HT containing neurons (Allers and Sharp 2003; Hajos et al. 2007). The DRN neurons we recorded with

a “classical” serotonin neuron profile(Aghajanian and Vandermaelen 1982; Trulson and Jacobs 1979) exhibited diverse behavioral response profiles and we observed little correlation between behavioral responses and most firing properties (Fig. 8), as reported in the monkey DRN(Nakamura et al. 2008).

Distinct nuclei within the DRN have specific patterns of afferent and efferent connectivity (Hajos et al. 1998; Lee et al. 2007; Lee et al. 2008; Lowry et al. 2008; Peyron et al. 1998; Van Bockstaele et al. 1993; Zhuang et al. 2005) and this might also contribute to the heterogeneity of DRN responses. Most classical studies focused on midline neurons, which project to prefrontal areas(Aghajanian and Vandermaelen 1982; Fornal et al. 1996) whereas Nakamura et al. (2008) recorded from the lateral wings, which project to areas such as the superior colliculus and striatum (Janusonis et al. 1999). Our sample included both midline and lateral recording sites. Of the 41 neurons analyzed in this study, we were able to specify the locations of 23 neurons. Of these eight neurons were from the midline and fifteen from the lateral subdivisions. Response profiles for the two groups of neurons are summarized in Table 2. While we did not see any statistically significant differences between the two subdivisions, our small sample size is not sufficient for a rigorous test of this hypothesis.

DRN responses frequently showed a high degree of sensory specificity. Over one third of DRN neurons that were modulated during odor sampling were selectively tuned to specific odor stimuli (Fig. 4a,c). To our knowledge, this is the first demonstration that DRN neurons show specific sensory tuning. Sensory selectivity suggests a possible

mechanism for stimulus-specific forms of "top-down" modulatory control. For example, the DRN sends a very large projection to the olfactory bulb, where it may modulate the early olfactory sensory processing (Ranade and Mainen 2004).

More than half of recorded neurons responded to the "click" sound of the solenoid valve used to deliver water with an extremely rapid, transient response, peaking in as little as 20 ms, a latency lower than previously reported for auditory responses(Heym et al. 1982; Waterhouse et al. 2004), and comparable to that of responses observed in auditory cortex(Heil and Irvine 1997). This indicates that serotonin release may be capable of modulating even the earliest stages of cortical sensory processing. Indeed, the click-evoked transients might be related to suppression of processing of the solenoid noise, consistent with the involvement of 5-HT in the suppression of sensory responsivity(Hurley and Pollak 2001; Kayama et al. 1989; Waterhouse et al. 1990) and startle reflexes(Davis et al. 1980). Postsynaptic ionotropic 5-HT3 receptors with extremely rapid kinetics(Chameau and van Hooft 2006) represent an attractive mechanism for rapid readout of such 5-HT transients.

Many DRN neurons responded selectively to specific actions during the task action sequence (Fig. 3; 4b,d), even actions that shared general locomotor characteristics, e.g. nose pokes into different ports (Fig. 3b) but differed in the details of the motor pattern and context. DRN firing has previously been reported to correlate with locomotion (Fornal et al. 1996; Veasey et al. 1997; Waterhouse et al. 2004) and rhythmic behaviors(Fornal et al. 1996; Veasey et al. 1997). Previous studies have also documented

relatively specific motor correlates, e.g. oral-buccal movements associated with feeding but not yawning (Fornal et al. 1996; Veasey et al. 1997), and eye movements direction(Nakamura et al. 2008). However, these studies showed more tonic modulations (around 1 s) and were relatively sparse(Nakamura et al. 2008). The more robust and finer scale of temporal modulation we observed could be explained by the combination of stereotypy resulting from a well-learned behavior sequence (vs. freely behaving cats(Fornal et al. 1996; Veasey et al. 1997)) and greater range of motor activity due to the absence of restraint (vs. head fixed monkeys(Nakamura et al. 2008), c.f. (Kulichenko and Pavlenko 2004). Specific motor responses may be related to the activation of specific central pattern generators(Hattox et al. 2003; Schmidt and Jordan 2000), possibly on the time scale of individual cycles(Kepecs et al. 2007).

We frequently observed DRN neurons that were activated during both odor port and choice port entry and exit (motor facilitation), but were inhibited during odor sampling (sensory disinhibition and motor inhibition) (Fig. 3, 7). Moreover, the same DRN neurons that responded to the solenoid valve (discussed above) tended to show suppression during odor sampling (Fig. 7). These patterns of activity are reminiscent of the "motor hypothesis" proposed by Jacobs and colleagues (Jacobs and Fornal 1997). According to this proposal, DRN neuronal firing facilitates motor processes and inhibits sensory processes. Thus, periods of increased 5-HT firing are associated with movement and suppression of sensation, while decreased 5-HT activity is associated with movement cessation and enhancement of sensation.

In addition to frank sensory and motor responses we also observed a relatively large fraction of neurons responding during the reward phase of the task, as was reported previously(Nakamura et al. 2008). Phasic 5-HT signals have been theorized to report a negative error in reward prediction or an unexpected aversive outcome(Daw et al. 2002) and we tested this idea using reward omissions. Indeed, a small subset of neurons (4/32) responded to reward omission around the expected time of reward (Fig. 6). The relative scarcity might be attributable to a failure of the omissions to trigger behavioral adjustments. Interestingly, we also observed several examples of DRN neurons in which the temporal structure of firing rates was matched to the temporal expectation of reward in the absence of direct sensory cue or overt motor responses (Fig. 6a).

The diversity, specificity and precision of behavioral correlates we report demonstrate that the DRN receives substantial information relating to a wide variety of sensory and motor as well as reward-related events, and 5-HT neurons may access and broadcast this information. These findings reinforce the challenge of assembling a unity theory of 5-HT function and underline the importance of determining how informational diversity maps onto the anatomical and neurochemical diversity of the DRN and how transient firing of DRN neurons is read out by its widespread downstream targets.

REFERENCES

Aghajanian GK, and Vandermaelen CP. Intracellular recordings from serotonergic dorsal raphe neurons: pacemaker potentials and the effect of LSD. *Brain Res* 238: 463-469, 1982.

Aghajanian GK, Wang RY, and Baraban J. Serotonergic and non-serotonergic neurons of the dorsal raphe: reciprocal changes in firing induced by peripheral nerve stimulation. *Brain Res* 153: 169-175, 1978.

Allers KA, and Sharp T. Neurochemical and anatomical identification of fast- and slow-firing neurones in the rat dorsal raphe nucleus using juxtacellular labelling methods in vivo. *Neuroscience* 122: 193-204, 2003.

Aston-Jones G, and Cohen JD. An integrative theory of locus coeruleus-norepinephrine function: adaptive gain and optimal performance. *Annu Rev Neurosci* 28: 403-450, 2005.

Britten KH, Shadlen MN, Newsome WT, and Movshon JA. The analysis of visual motion: a comparison of neuronal and psychophysical performance. *J Neurosci* 12: 4745-4765, 1992.

Chameau P, and van Hooft JA. Serotonin 5-HT(3) receptors in the central nervous system. *Cell Tissue Res* 326: 573-581, 2006.

Cools R, Roberts AC, and Robbins TW. Serotoninergic regulation of emotional and behavioural control processes. *Trends Cogn Sci* 12: 31-40, 2008.

Davis M, Strachan DI, and Kass E. Excitatory and inhibitory effects of serotonin on sensorimotor reactivity measured with acoustic startle. *Science* 209: 521-523, 1980.

Daw ND, Kakade S, and Dayan P. Opponent interactions between serotonin and dopamine. *Neural Netw* 15: 603-616, 2002.

Dayan P, and Huys QJ. Serotonin, inhibition, and negative mood. *PLoS Comput Biol* 4: e4, 2008.

Deakin JF, and Graeff FG. 5-HT and mechanisms of defence. *Journal of Psychopharmacology* 5: 305-315, 1991.

Descarries L, Watkins KC, Garcia S, and Beaudet A. The serotonin neurons in nucleus raphe dorsalis of adult rat: a light and electron microscope radioautographic study. *J Comp Neurol* 207: 239-254, 1982.

Doya K. Metalearning and neuromodulation. *Neural Netw* 15: 495-506, 2002.

Feierstein CE, Quirk MC, Uchida N, Sosulski DL, and Mainen ZF. Representation of spatial goals in rat orbitofrontal cortex. *Neuron* 51: 495-507, 2006.

Fornal CA, Metzler CW, Marrosu F, Ribiero-do-Valle LE, and Jacobs BL. A subgroup of dorsal raphe serotonergic neurons in the cat is strongly activated during oral-buccal movements. *Brain Res* 716: 123-133, 1996.

Green DM, and Swets JA. *Signal detection theory and psychophysics*. New York: Wiley, 1966.

Hajos M, Allers KA, Jennings K, Sharp T, Charette G, Sik A, and Kocsis B. Neurochemical identification of stereotypic burst-firing neurons in the rat dorsal raphe nucleus using juxtacellular labelling methods. *Eur J Neurosci* 25: 119-126, 2007.

Hajos M, Richards CD, Szekely AD, and Sharp T. An electrophysiological and neuroanatomical study of the medial prefrontal cortical projection to the midbrain raphe nuclei in the rat. *Neuroscience* 87: 95-108, 1998.

Hattox A, Li Y, and Keller A. Serotonin regulates rhythmic whisking. *Neuron* 39: 343-352, 2003.

Heil P, and Irvine DR. First-spike timing of auditory-nerve fibers and comparison with auditory cortex. *J Neurophysiol* 78: 2438-2454, 1997.

Heym J, Trulson ME, and Jacobs BL. Raphe unit activity in freely moving cats: effects of phasic auditory and visual stimuli. *Brain Res* 232: 29-39, 1982.

Hurley LM, and Pollak GD. Serotonin effects on frequency tuning of inferior colliculus neurons. *J Neurophysiol* 85: 828-842, 2001.

Jacobs BL, and Azmitia EC. Structure and function of the brain serotonin system. *Physiol Rev* 72: 165-229, 1992.

Jacobs BL, and Fornal CA. Serotonin and motor activity. *Curr Opin Neurobiol* 7: 820-825, 1997.

Janusonis S, Fite KV, and Foote W. Topographic organization of serotonergic dorsal raphe neurons projecting to the superior colliculus in the Mongolian gerbil (Meriones unguiculatus). *J Comp Neurol* 413: 342-355, 1999.

Kayama Y, Shimada S, Hishikawa Y, and Ogawa T. Effects of stimulating the dorsal raphe nucleus of the rat on neuronal activity in the dorsal lateral geniculate nucleus. *Brain Res* 489: 1-11, 1989.

Kepecs A, Uchida N, and Mainen ZF. Rapid and precise control of sniffing during olfactory discrimination in rats. *J Neurophysiol* 98: 205-213, 2007.

Kulichenko AM, and Pavlenko VB. Self-Initiated Behavioral Act-Related Neuronal Activity in the Region of the Raphe Nuclei of the Cat. *Neurophysiology* 36: 50-57, 2004.

Lee HS, Eum YJ, Jo SM, and Waterhouse BD. Projection patterns from the amygdaloid nuclear complex to subdivisions of the dorsal raphe nucleus in the rat. *Brain Res* 1143: 116-125, 2007.

Lee SB, Lee HS, and Waterhouse BD. The collateral projection from the dorsal raphe nucleus to whisker-related, trigeminal sensory and facial motor systems in the rat. *Brain Res* 1214: 11-22, 2008.

Lowry CA, Evans AK, Gasser PJ, Hale MW, Staub DR, and Shekhar A. *Topographic organization and chemoarchitecture of the dorsal raphe nucleus and the median raphe nucleus*. Birkhäuser, 2008, p. 25-67.

McGinty DJ, and Harper RM. Dorsal raphe neurons: depression of firing during sleep in cats. *Brain Res* 101: 569-575, 1976.

Michelsen KA, Schmitz C, and Steinbusch HW. The dorsal raphe nucleus--from silver stainings to a role in depression. *Brain Res Rev* 55: 329-342, 2007.

Montagne-Clavel J, Oliveras JL, and Martin G. Single-unit recordings at dorsal raphe nucleus in the awake-anesthetized rat: spontaneous activity and responses to cutaneous innocuous and noxious stimulations. *Pain* 60: 303-310, 1995.

Nakamura K, Matsumoto M, and Hikosaka O. Reward-dependent modulation of neuronal activity in the primate dorsal raphe nucleus. *J Neurosci* 28: 5331-5343, 2008.

Peyron C, Petit JM, Rampon C, Jouvet M, and Luppi PH. Forebrain afferents to the rat dorsal raphe nucleus demonstrated by retrograde and anterograde tracing methods. *Neuroscience* 82: 443-468, 1998.

Ranade SP, and Mainen ZF. Serotonin modulates odor-evoked sensory input in the rat main olfactory bulb. In: *Society for Neuroscience*. San Diego: 2004.

Richerson GB. Serotonergic neurons as carbon dioxide sensors that maintain pH homeostasis. *Nat Rev Neurosci* 5: 449-461, 2004.

Schmidt BJ, and Jordan LM. The role of serotonin in reflex modulation and locomotor rhythm production in the mammalian spinal cord. *Brain Res Bull* 53: 689-710, 2000.

Schultz W. Multiple dopamine functions at different time courses. *Annu Rev Neurosci* 30: 259-288, 2007.

Schultz W, Dayan P, and Montague PR. A neural substrate of prediction and reward. *Science* 275: 1593-1599, 1997.

Soubrie P. Reconciling the role of central serotonin neurons in human and animal behavior. *Behav Brain Sci* 9: 319-364, 1986.

Tecott LH. Serotonin and the orchestration of energy balance. *Cell Metab* 6: 352-361, 2007.

Trulson ME, and Jacobs BL. Raphe unit activity in freely moving cats: correlation with level of behavioral arousal. *Brain Res* 163: 135-150, 1979.

Uchida N, and Mainen ZF. Speed and accuracy of olfactory discrimination in the rat. *Nat Neurosci* 6: 1224-1229, 2003.

Urbain N, Creamer K, and Debonnel G. Electrophysiological diversity of the dorsal raphe cells across the sleep-wake cycle of the rat. *J Physiol* 573: 679-695, 2006.

Van Bockstaele EJ, Biswas A, and Pickel VM. Topography of serotonin neurons in the dorsal raphe nucleus that send axon collaterals to the rat prefrontal cortex and nucleus accumbens. *Brain Res* 624: 188-198, 1993.

Veasey SC, Fornal CA, Metzler CW, and Jacobs BL. Response of serotonergic caudal raphe neurons in relation to specific motor activities in freely moving cats. *J Neurosci* 15: 5346-5359, 1995.

Veasey SC, Fornal CA, Metzler CW, and Jacobs BL. Single-unit responses of serotonergic dorsal raphe neurons to specific motor challenges in freely moving cats. *Neuroscience* 79: 161-169, 1997.

Waterhouse BD, Azizi SA, Burne RA, and Woodward DJ. Modulation of rat cortical area 17 neuronal responses to moving visual stimuli during norepinephrine and serotonin microiontophoresis. *Brain Res* 514: 276-292, 1990.

Waterhouse BD, Devilbiss D, Seiple S, and Markowitz R. Sensorimotor-related discharge of simultaneously recorded, single neurons in the dorsal raphe nucleus of the awake, unrestrained rat. *Brain Res* 1000: 183-191, 2004.

Zhuang X, Masson J, Gingrich JA, Rayport S, and Hen R. Targeted gene expression in dopamine and serotonin neurons of the mouse brain. *J Neurosci Methods* 143: 27-32, 2005.

Figure legends

Figure 1: Neurons in the dorsal raphe nucleus exhibit state dependent modulation.

(**a**) Schematic diagram of recording strategy. Cartoon of coronal section of rat brain at the level of the DRN with attached guide cannula and micro-drive with tetrodes. Guide cannula was inserted into the brain and tetrodes were gradually lowered through the cannula to the DRN.

(**b**) Inset in **a** is magnified. Shaded grey area shows extent of the DRN (DR) and recording area. aq, cerebral aqueduct; pag, periaqueductal gray.

(**c**) Histological verification of tetrode track. Coronal section of the rat brain with a single tetrode track passing through the DRN observed by fluorescence imaging of DiI (red).

(**d**) Extracellular spike waveforms of 52 neurons recorded from DRN of 7 rats. Neurons in orange are classified as wide spiking neurons (WS) and narrow spiking neurons are in blue (NS) (S1a). Neuron marked with black circle is an example of a "classical" wide spiking putative 5-HT neuron. Numbers next to waveform indicate neuron ID.

(**e**) State dependent modulation of firing rate of WS neuron marked in **d**. *Top panel*: Spectrogram of hippocampal LFP. *Middle panel* shows timing of task events (black line) and classification into Sleep (Blue), Task Engaged (Green) and Awake (Red) behavioral states. *Lower panel* shows the binned firing rate for the neuron. Firing rate of the neuron is lowered during sleep.

(**f**) Average firing rates during the three behavioral states for neuron in **e**. Firing rate decreases during sleep compared to the awake state and remains unchanged during the task state.

(**g**) Sleep index is plotted as function of spike width. Most neurons show suppression of firing during sleep. There is no significant correlation between sleep index and spike width. Black line is the best fit line and R^2 is the coefficient of correlation. Black circle denotes neuron shown in **d-f**.

(**h**) Task index is plotted as function of spike width.

Figure 2: Firing patterns of DRN neurons during 2-odor discrimination task.

(**a**) Schematic diagram of the timing of behavioral events during an example trial. Timing of behavioral events is recorded using the interruption of the infrared photobeam inside the ports (odor and water ports) and odor and water are delivered via computer controlled valves. An example of all major events during a correct trial is shown.

(**b**) Normalized firing rates for all recorded neurons aligned to all behavioral events during the task. Pseudocolor plot shows peri-event firing rate modulation of 52 neurons recorded during the task with firing rates scaled from zero to maximum firing rate during the task for each neuron. Neurons are sorted by increasing average firing rate during the Task epoch. Numbers to the left indicate neuron IDs and correspond to **Fig. 1d**. Neuron

IDs in red were excluded from subsequent analyses on account of low overall firing rates. Neuron with asterisk is same as in **Fig. 1**. Black line segments at the bottom show fixed 300ms peri-event behavioral epochs.

(**c**) Number of neurons modulated during task. Number of neurons showing significant ROC modulation index (RMI, $P < 0.01$) during five behavioral epochs depicted in **b**. Inhibitory responses (red) and excitatory responses (green) are shown separately.

(**d**) Many DRN neurons modulate their firing rate during more than one epoch. Bar graph shows number of neurons as function of number of epochs that show significant firing rate modulation. Epochs are the same as in **b,c**.

(**e-f**) Strongest transient modulation during behavioral epochs is not correlated with state dependent modulation during sleep (**e**) and width of spike waveform (**f**). Black circle marks WS neuron shown in **Fig. 1,2b**. Color code is identical to **Fig. 1d**. Black line is the best fit line and R^2 is the coefficient of correlation.

Figure 3: Correlates of task actions in raphe neurons.

Rasters and peri-stimulus time histograms (PSTH) are plotted during execution of various task actions. (*Top*) Schematic of trial structure and relevant behavioral events. (*Inset*) Raster plot represents neuronal activity in individual trials (rows); each tick mark represents a spike. Timing of spikes is relative to behavioral event in seconds. PSTH is

binned with a time window of 15 ms and smoothed with a Gaussian filter of standard deviation 30 ms. Twenty randomly chosen trials are plotted for each raster. Green dashed line indicates average firing rate during Task Engaged (T) state. For all PSTH plots, the shaded area is ± S.E.M.

(**a**) Example of neuron that responds during approach to both odor and water port. Only correct trials are plotted. *Left panel* shows raster and PSTH aligned to entry into odor port. Blue ticks indicate time of exit from the odor port. Trials are sorted by duration of stay within the odor port. *Right panel* shows same neuron with firing aligned to entry into water port.

(**b**) Example of neuron that responds selectively during approach to odor port but not to water port. Blue ticks in left panel indicate odor port exit.

(**c**) Example of neuron responding to withdrawal from water port but not the odor port. *Left panel* shows raster-PSTH aligned to exit from odor port and *right panel* is aligned exit from water port.

(**d**) Example of selective suppression of firing at odor port. *Left panel* is aligned to odor port entry. Trials shown on raster are sorted by time of exit from the odor port (blue ticks). *Right panel* shows response of same neuron at the water port.

Figure 4: Specificity of tuning of raphe neurons.

(**a**) Example of an odor selective neuron. The two odors are air mixtures of enantiomers of 2-Octanol. Rasters and PSTH are aligned to onset of odor presentation. Trials in raster are sorted by duration of odor sampling (blue ticks indicate time of exit from odor port). Color of sidebar indicates trials in which S(+)-2-Octanol (blue) or R(-)-2-Octanol (green) were presented. This neuron was activated by S(+)-2-Octanol. Black bar above raster indicates fixed 300ms time window used for ROC analysis.

(**b**) Example of a direction selective neuron. Raster and PSTH are aligned on exit from odor port. Trials are grouped by direction of movement and sorted by duration of movement to the water port (blue ticks indicate time of entry into water port). Only trials with correct responses are included. Trials with movement to left port are indicated by golden sidebar while movement to right port by purple sidebar. This neuron responds to leftward movement.

(**c**) Population histogram of odor preference index. Preference index was calculated using an ROC analysis (see Experimental Procedures) during odor sampling epoch indicated in A to quantify selectivity of firing to one of the two odors. Colored bars indicate significant selectivity with $P < 0.01$ based on a permutation procedure; blue, cells selective for S(+)-2-Octanol; green, cells selective for R(-)-2-Octanol. Gray bars, not significant. Asterisk indicates preference value for example neuron shown in **a**.

(**d**) Population histogram of direction preference. Direction (Left/Right) selectivity was calculated during movement epoch indicated in **b**. Colored bars indicate significant direction preference ($P<0.01$); violet, selective for movement in rightward direction;

golden, selective for leftward direction; grey, not significant ($P < 0.01$). Asterisk indicates example neuron shown in **b**.

Figure 5: Water valve click responses.

(**a**) Example of click responsive neuron. Raster-PSTH is aligned to water valve onset (blue ticks represent water valve switch off time).

(**b**) Click versus tone responses. Latency of the peak of the sound evoked response is plotted against strength of the response. Neurons tested with clicks are plotted in blue while those tested with pure tone are plotted in red. Pure tone did not evoke strong, short latency responses as evoked by the click. Neuron shown in **a** is marked by an asterisk.

(**c**) Average click and tone evoked response. Average, normalized PSTH aligned to onset of valve click sound (blue, n = 23 neurons), and aligned to onset of pure tone (red, n = 18 neurons). Shaded area represents the ± S.E.M.

Figure 6: Reward correlates of raphe neurons.

(**a-b**) Neuronal responses are correlated with reward variables. Spikes are aligned to entry into water port. Trials with correct responses are grouped by water delivery (blue) or omission (pink). Trials are sorted by the duration of stay in the water port. Blue ticks

indicate time of exit from the water port. Both trial types were randomly interleaved in the session. Distribution of reward delays for the behavioral session is shown as a box plot with the red line denoting the median and the box denoting the inter quartile range. (**a**) Example neuron encoding reward delay. This neuron shows a monotonic decline in firing rate upon entry into water port. Firing rate reaches its minimum around the time of water delivery. This neuron also responds to the offset of water delivery in the reward delivered trials (blue). (**b**) Example neuron responding to reward omission. This neuron shows an increase in firing rate for trials where water was omitted (pink). Increase in firing rate precedes exit from the water port (blue ticks).

(**c**) A small subset of neurons responds to reward omission. *Top panel*; Sliding ROC preference analysis was performed on 50 ms time windows to compare firing rates between correct trials where water was delivered with those where water was omitted. Time intervals with significant preference values are plotted in pseudo color. Red intervals indicate increased firing during water delivery ('Reward preference') while blue intervals indicate increased firing during water omission trials ('omission preference'). Neurons shown in **a** and **b** and **S5** (Cell no. 20, 26) are indicated on the right. *Bottom panel* shows number of neurons at each time interval that prefer delivery or omission. Omission preference neurons are represented in blue while reward preference neurons are in red. A small subset of neurons shows significant omission preference that emerges after the time of expected reward.

Figure 7: Multiplicity of responses of DRN neurons.

(**a**) Example of neuron showing odor port inhibition, movement excitation and water valve click response. *Left panel* is aligned to entry into odor port, *middle panel* aligned to exit from the odor port and *right panel* aligned to water valve onset. Only correct trials are shown.

(**b**) z-score analysis. Normalized z-scores (see Experimental Procedures) plotted for all neurons recorded with an audible water valve click. Each row is a single neuron. z-scores of firing rates are plotted in pseudocolor. Panel alignments are identical to **a**. Neurons are ordered by their average z-score values during the odor sampling epoch. Neuron shown in A is indicated by an asterisk. Many neurons that are inhibited during odor sampling are also excited during movement and show a phasic click-evoked response. Color bar: z-score.

Fig. 8. Relationship between behavioral correlates and firing properties.

(**a-c**) Modulation of firing rates during behavior is not correlated with spike width. ROC modulation index (RMI) for all neurons plotted as a function of spike width during three behavioral epochs i.e. odor sampling, movement, and reward. Significant RMI values ($P<0.01$, Experimental Procedures) are shown for enhancement of firing (green) and suppression (red) compared to firing rate during the baseline while non-significant values are shown in grey.

Table 1. Percentages of DRN neurons modulated during selective task actions.

Table 1a shows the percentages of neurons significantly modulated ($P<0.01$) during port approach while Table 1b shows percentages during port withdrawal. Also included are actual numbers of neurons showing suppression or enhancement.

Table 2. Responses of midline and lateral wing DRN neurons.

Table 2 compares a set of responses of midline and lateral subdivision DRN neurons. Approach. There was no significant dependence between anatomical location and presence or absence of response as calculated by two-tailed Fischer exact test at $P<0.05$.

Supplementary Figure Legends

Figure S1: State dependent modulation of firing rates.

(**a**) Classification of DRN neurons by spike width. Spike width is defined as the time from positive peak of the spike waveform to the return to baseline. Peak-valley ratio, which is a measure of symmetry of the spike waveform, is the ratio of the amplitude of the positive and negative peaks. Peak-valley ratio is plotted as a function of the spike width. Neurons with spike width greater than 1.2 ms are grouped as wide spiking (WS)

neurons (orange), while the rest are grouped as narrow spiking (NS) neurons (blue). Most WS neurons also have an asymmetric spike waveform with a large peak and small valley.

(**b-c**) Firing properties of raphe neurons are not correlated with spike width. Average firing rate in the awake state (B) and firing rate variability as measured by CV2 (C) is plotted as a function of spike width. Black circle indicates neuron in **Fig. 1, 2**.

Figure S2: Relationship between state dependent modulation and neuronal firing properties.

Indices of state dependent modulation, sleep index and task index are compared with neuronal firing properties, average firing rate and firing rate variability (CV2). (**a-b**) shows plots of sleep index as a function of firing rate (**a**) and CV2 (**b**). Black line is the line of best fit. R^2 is coefficient of cross-correlation. (**c-d**) show plots for task index with firing rate and CV2 respectively. Only task index and CV2 are significantly correlated at $P < 0.01$.

Figure S3: Relationship between strength of transient task event related modulation and neuronal firing properties.

Strongest behavioral epoch modulation for each neuron during five fixed epochs spanning the entire task (**Fig. 2d**) is compared to firing rate (**a**) and spike train variability

(CV2) (**b**). Color code is same as in **S2**. Firing rate shows a significant positive correlation with modulation strength while CV2 (spike train variability) is not correlated. Black line is the line of best fit.

Figure S4: Two types of phasic click evoked responses

(**a**) Example of neuron with very short latency click evoked response. Raster-PSTH are aligned to onset of water valve and grouped by water delivery (blue sidebar) and water omission (pink). In case of omitted trials, there was no click sound. Spontaneous firing rate of neuron is low; however in response to the click, the neuron fires a burst of spikes at very short latency.

(**b**) Example of a neuron with spike reorganization in response to click. Raster and PSTH are grouped for trials where click was presented (blue, water delivered trials) and where click was not presented (pink, water omitted trials). Click evoked response for this neuron (same as in **Fig. 5a**) is followed by a suppression of firing rate. Suppression is absent when the click is not presented. Overall increase in firing rate is not as pronounced as in (**a**).

Figure S5: Responses to reward structure

(**a-b**) Example neurons showing differential firing in response to omission of reward. Raster and PSTH are plotted for trials where water was delivered (blue) and where water was omitted (pink). Box plot above PSTH shows distribution of water delivery times during the session. Red line in box plot indicates median time of water delivery. (**a**) Firing rate of neuron increases immediately upon water delivery while omission of water leads to sustained suppression of firing. This neuron also shows sustained firing during the reward delay. Neuron in (**b**) shows opposite modulation with sustained suppression of firing following water delivery and increase in firing rate upon omission of water. ROC preference analysis for the two neurons is seen in **Fig. 6c**.

Figure S6: Behavioral responses are independent of firing rate and variability

ROC modulation index (RMI) is not correlated with basic firing properties of DRN neurons. Modulation of firing rate during three task epochs (same as **Fig. 8**) is plotted against firing rate (**a-c**) and CV2 (**d-f**). Significant RMI values (permutation procedure, at $P<0.01$ see Experimental procedures) are plotted in color. Solid green circles denote increase in firing during the epoch, while red denotes decreased firing rate. Significantly modulated units are spread along the entire range of the independent variables, namely firing rate and CV2.

Tables

Table 1a. Modulation of firing rates during port approach

Type of modulation	Enhancement	Suppression	Total	Percentage of modulated neurons (%)
Odor port approach only	4	1	5	12.2
Water port approach only	2	3	5	12.2
Both odor and water approach	14	1	15	36.6
Opposite tuning at both ports	1	3	4	9.7
No approach related modulation	-	-	12	29.3
Total number of neurons	21	8	41	

Table 1b. Modulation of firing rates during port withdrawal

Type of modulation	Enhancement	Suppression	Total	Percentage of modulated neurons (%)
Odor port withdrawal only	7	1	8	20
Water port withdrawal only	1	2	3	7.5
Both odor and water withdrawal	10	2	12	30
Opposite tuning at both ports	3	3	6	15
No withdrawal related modulation	-	-	11	27.5
Total number of neurons	21	8	40	

Table 2. Responses of midline and lateral wing DRN neurons

Type of modulation	Midline (n=8)	Lateral (n=15)
Odor port inhibition	1	1
Odor response	3	7
Movement response	3	9
Odor selectivity	2	6
Direction selectivity	1	6
Click response	3	9

Figure -1 (Mainen)

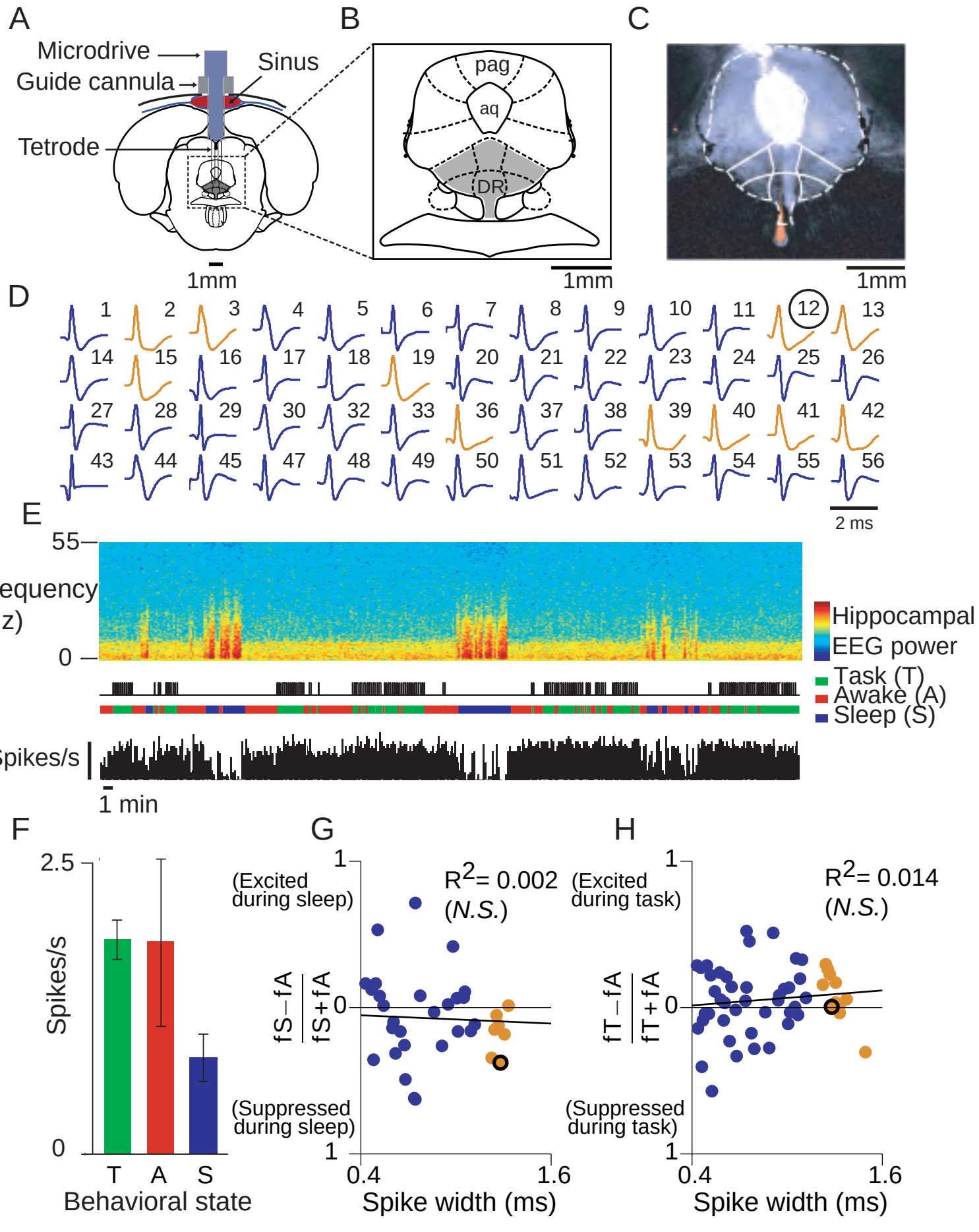

Figure - 2 (Mainen)

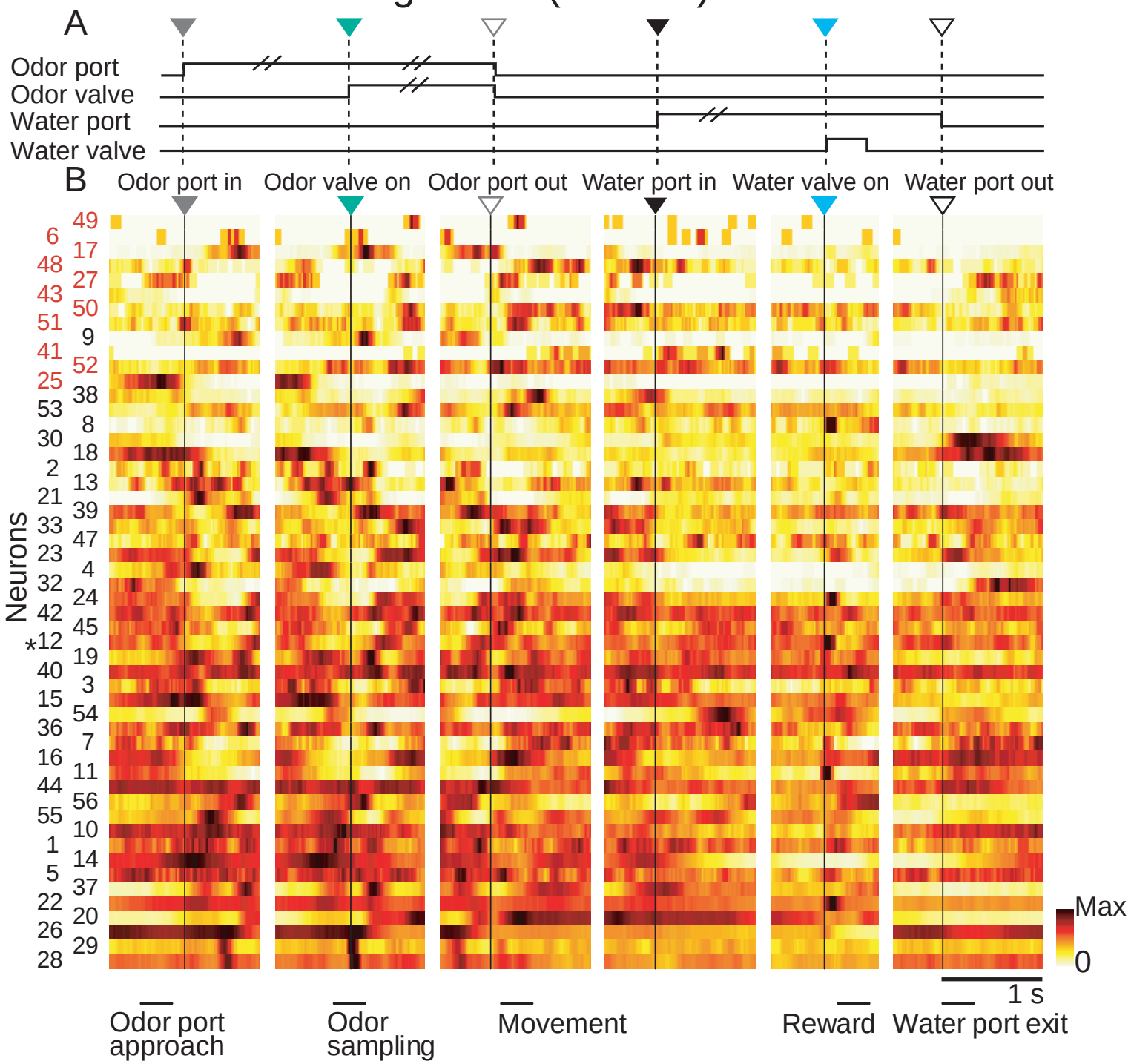

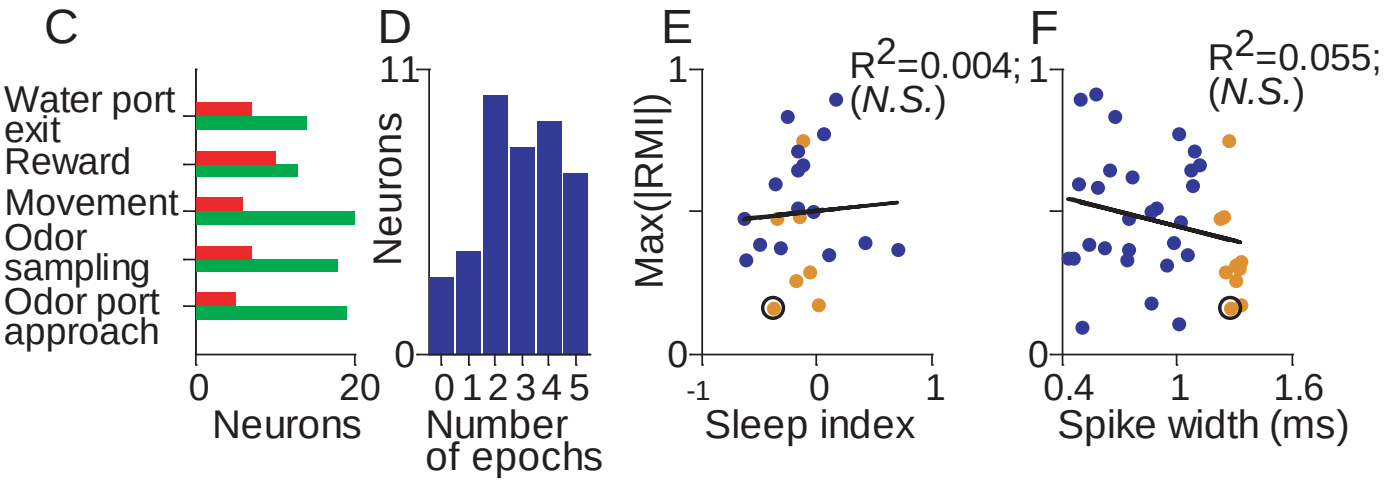

Figure - 3 (Mainen)

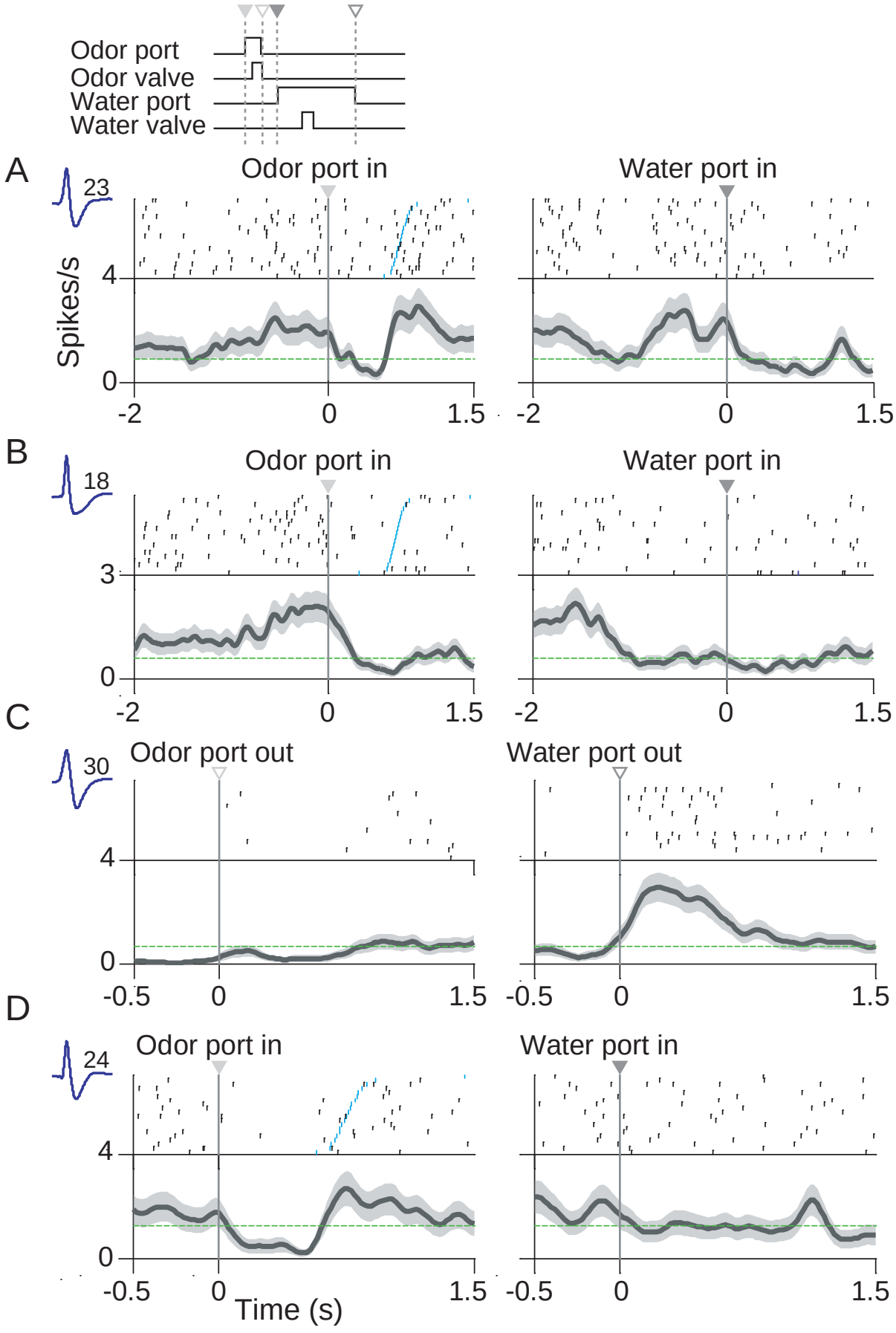

Figure - 4 (Mainen)

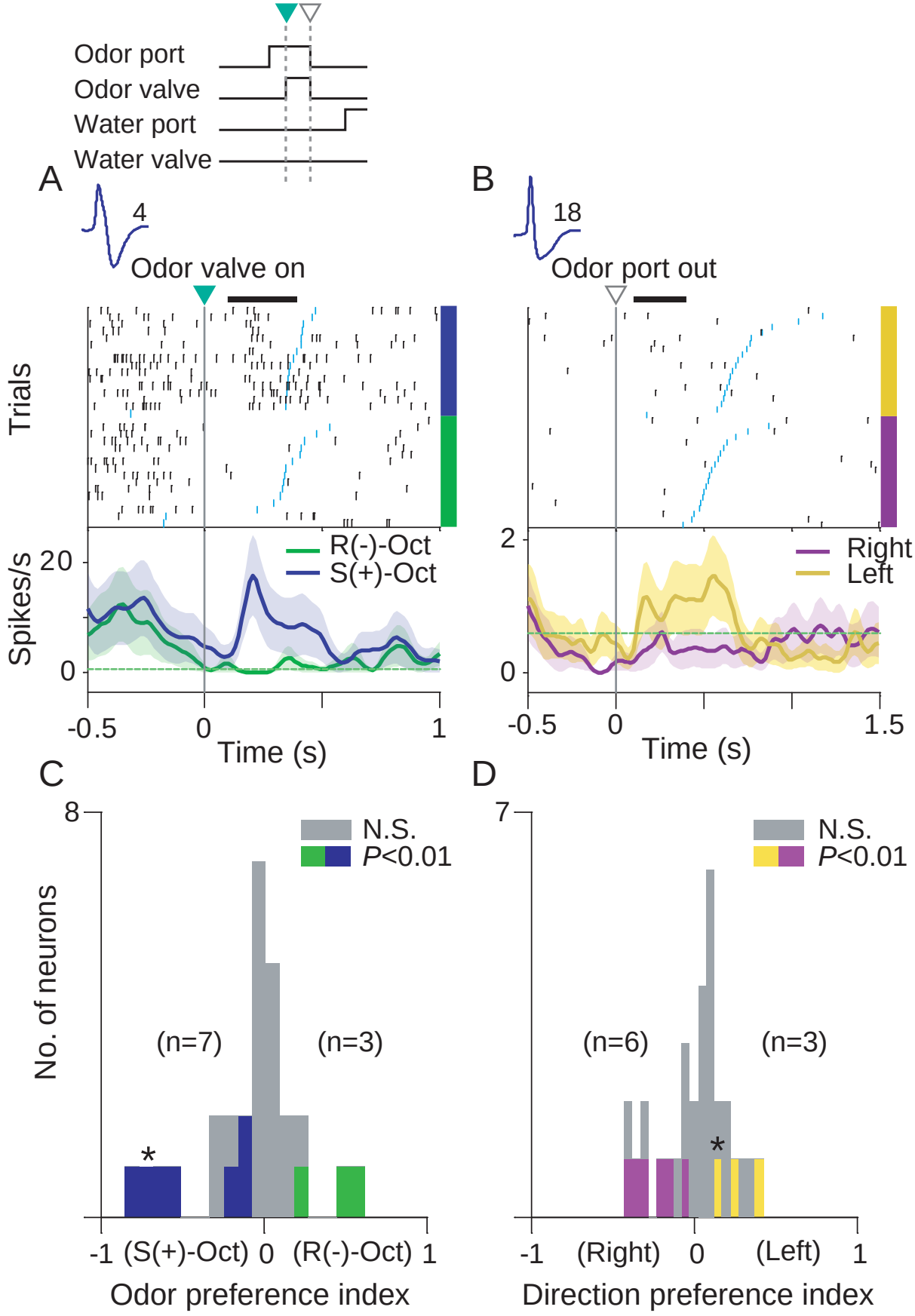

Figure - 5 (Mainen)

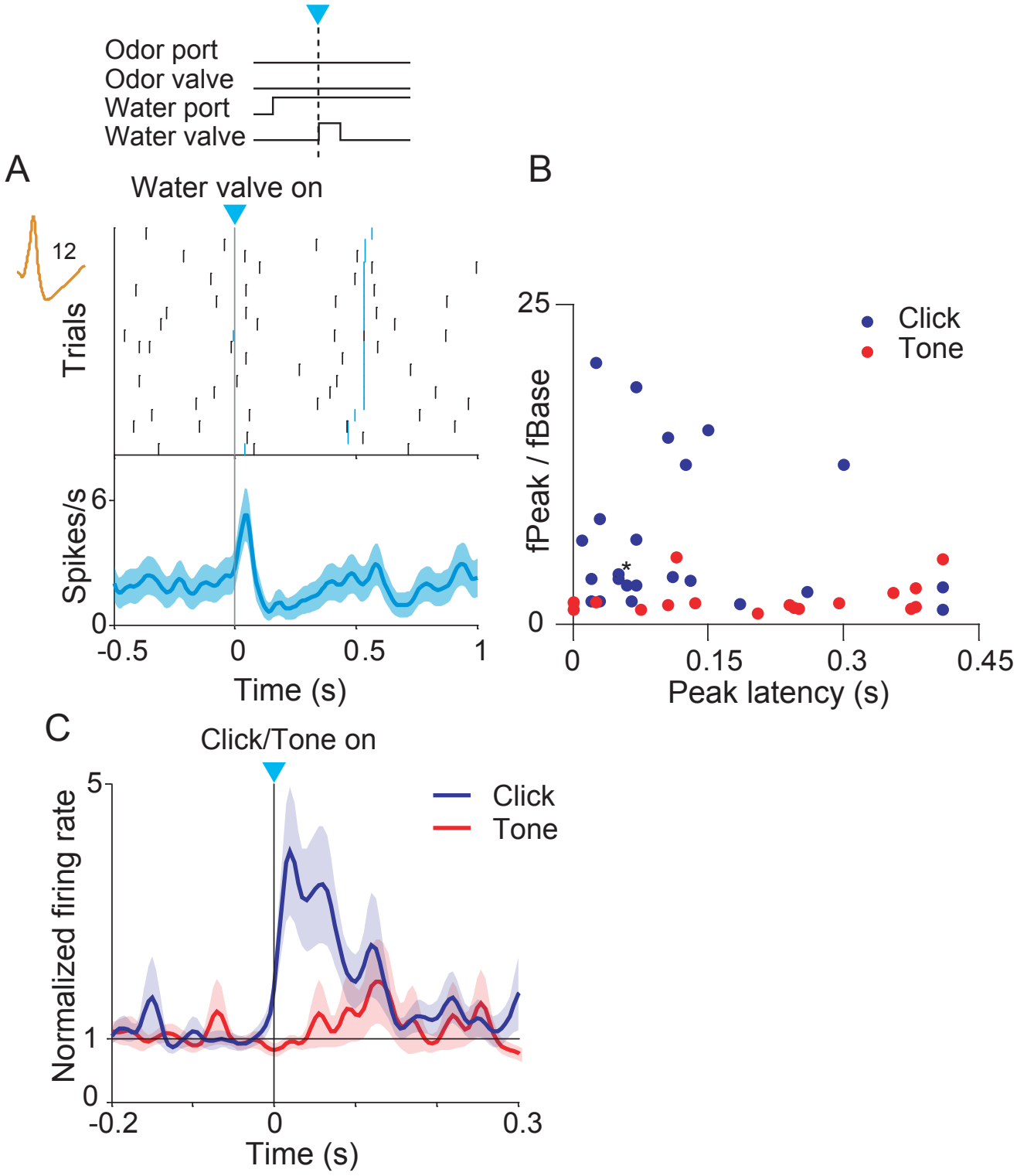

Figure - 6 (Mainen)

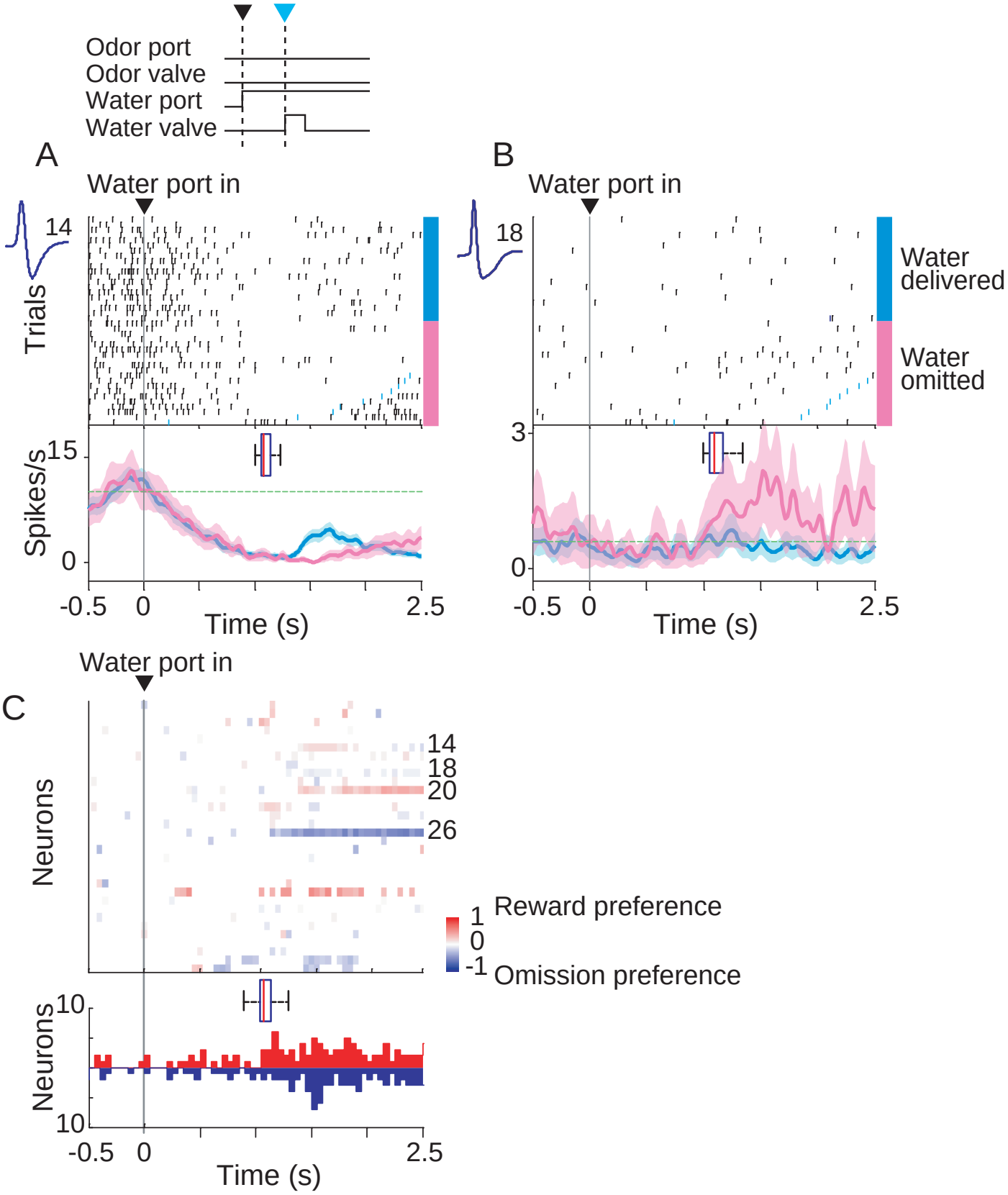

Figure - 7 (Mainen)

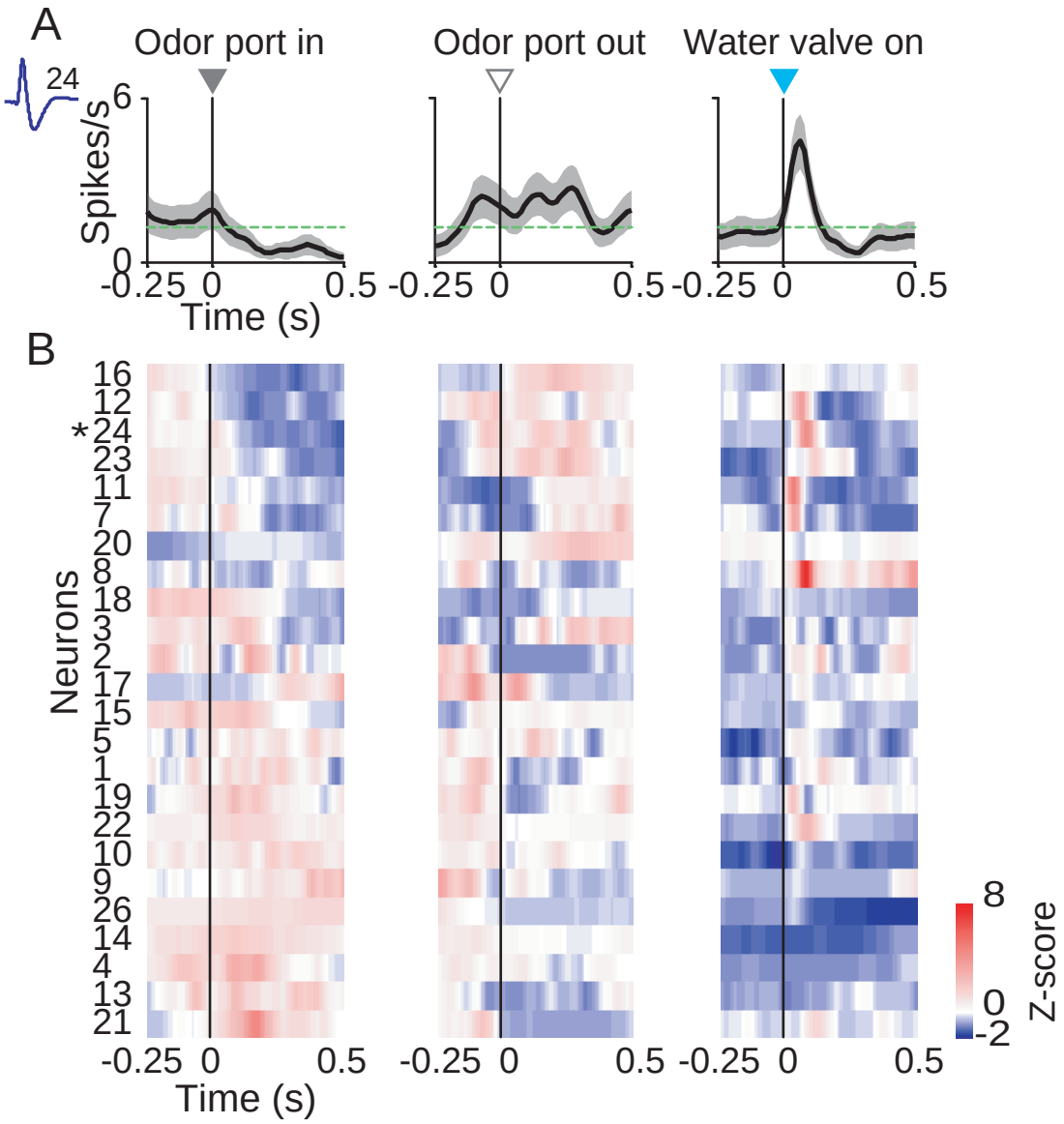

Figure - 8 (Mainen)

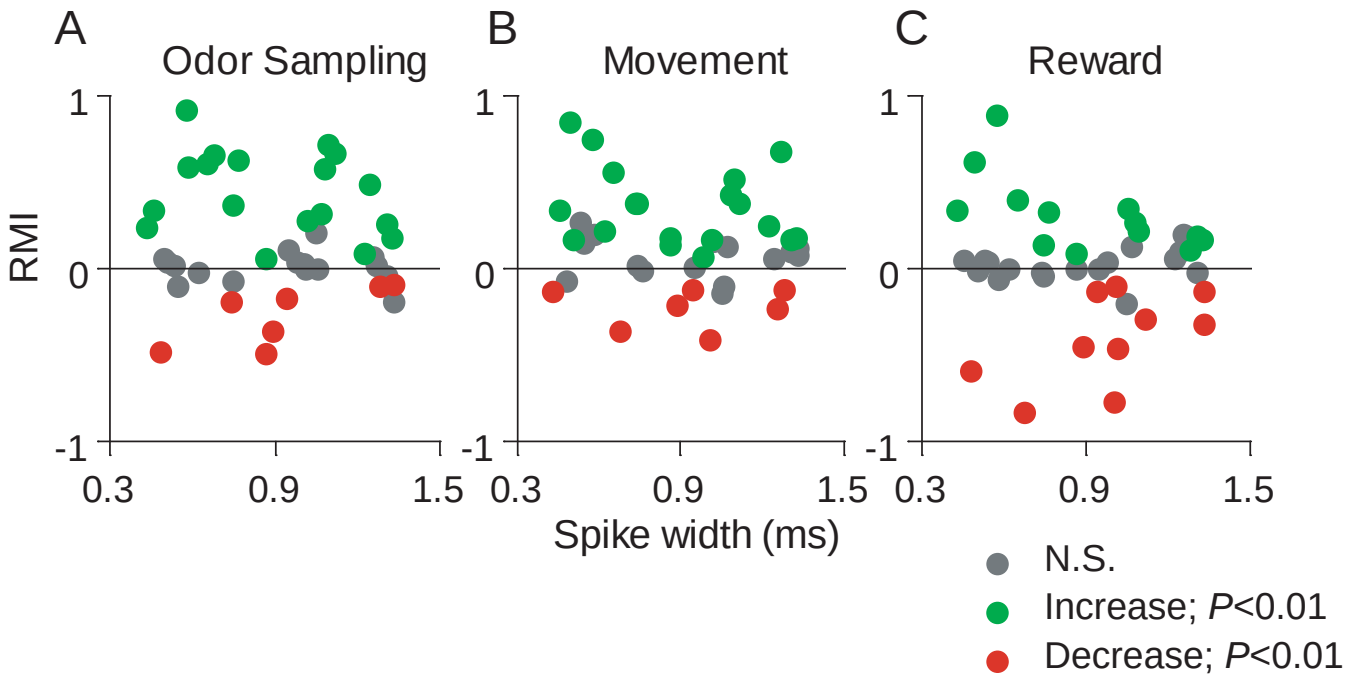

Supplementary figure - 1 (Mainen)

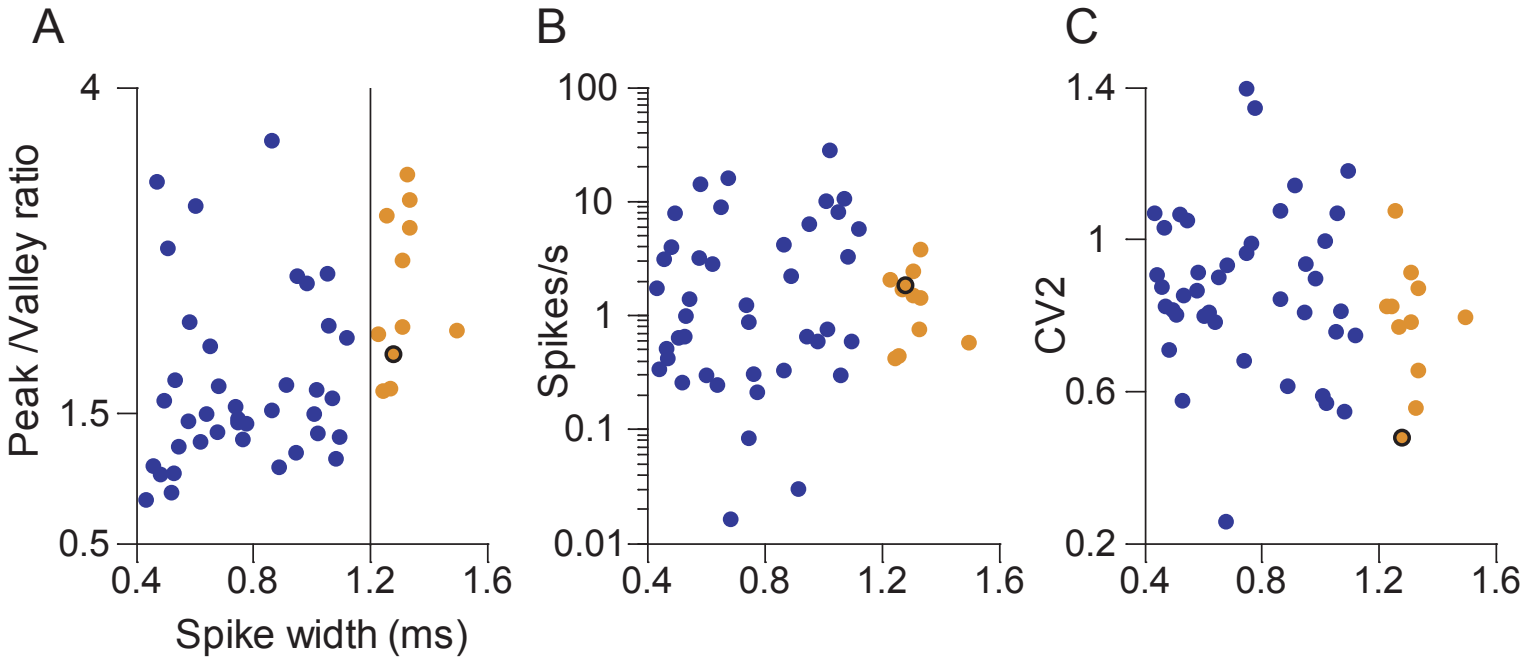

Supplementary figure - 2 (Mainen)

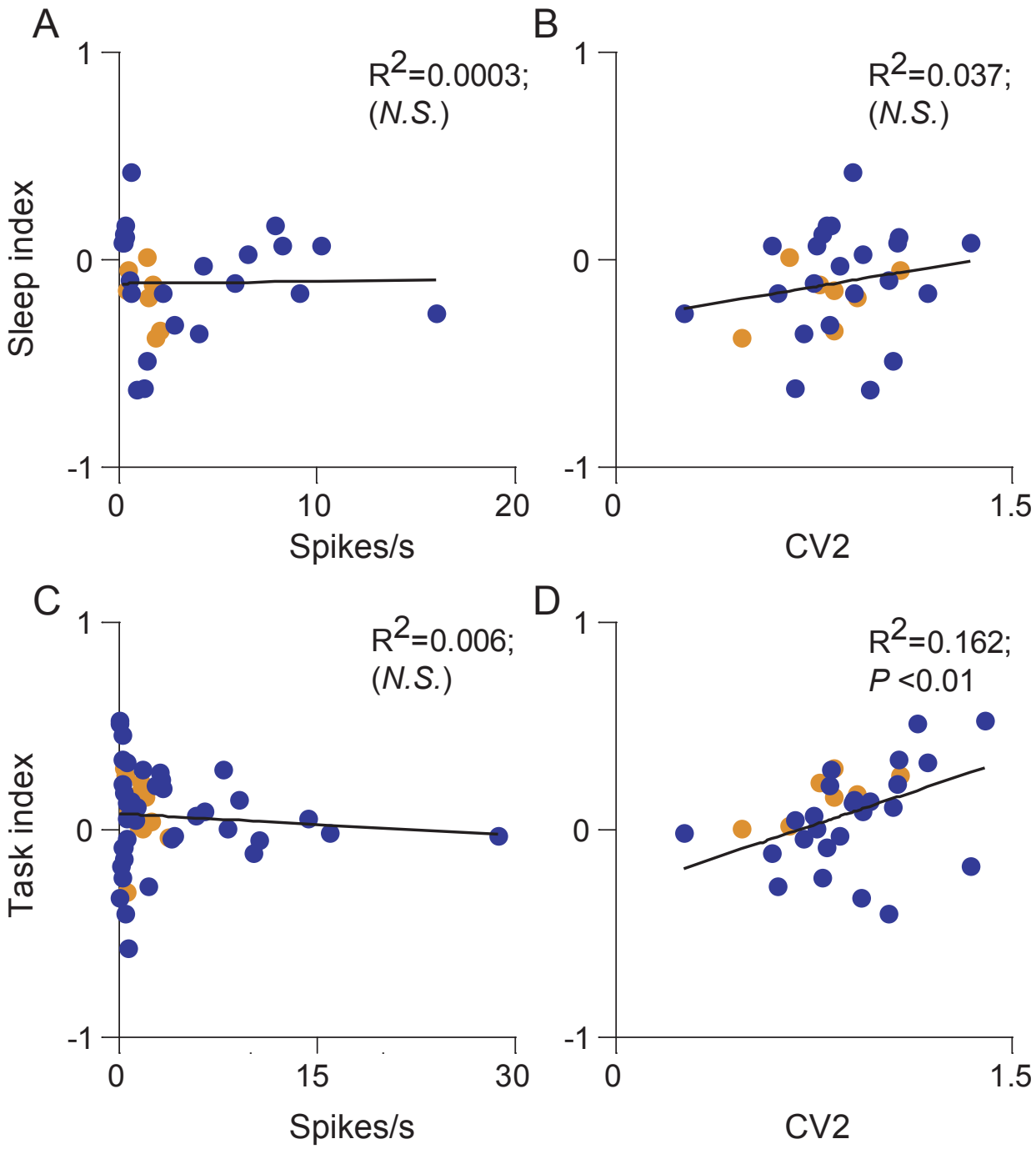

Supplementary figure - 3 (Mainen)

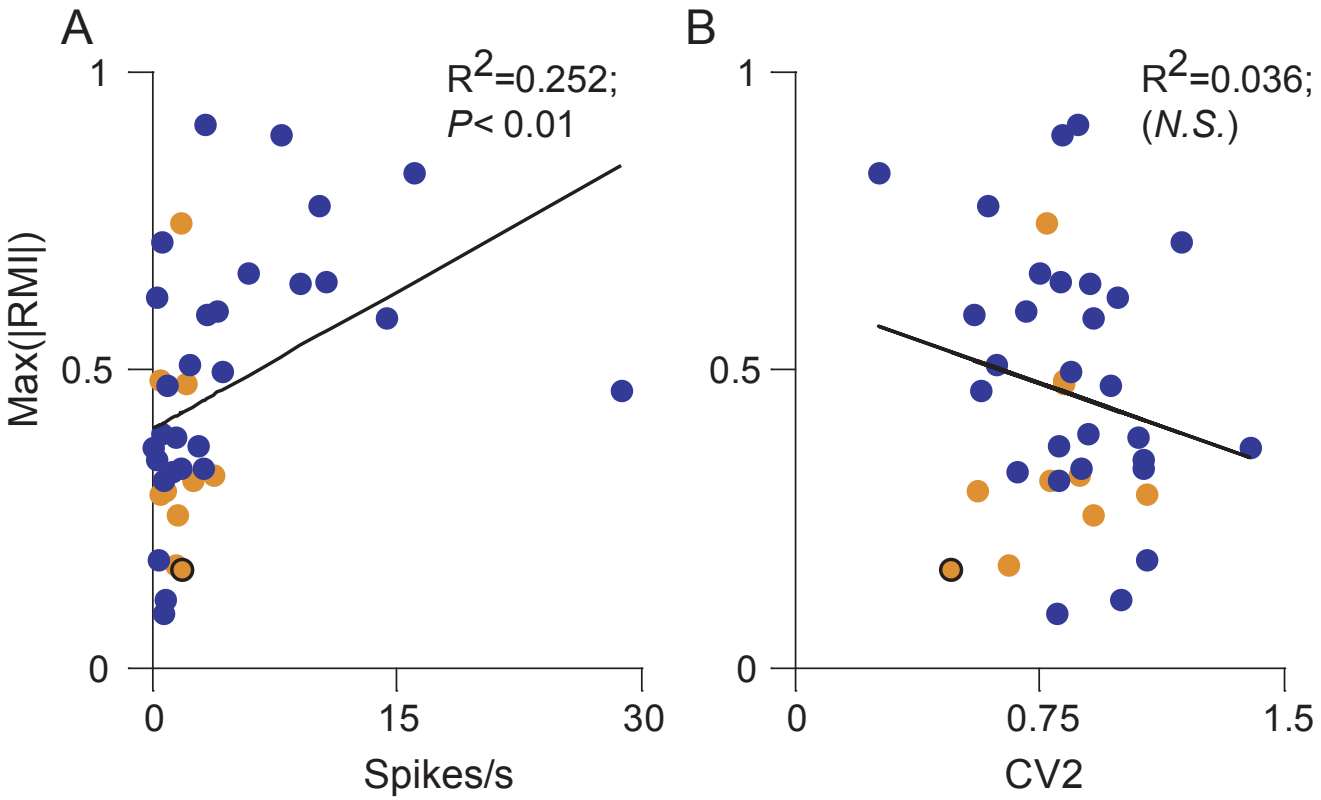

Supplementary figure - 4 (Mainen)

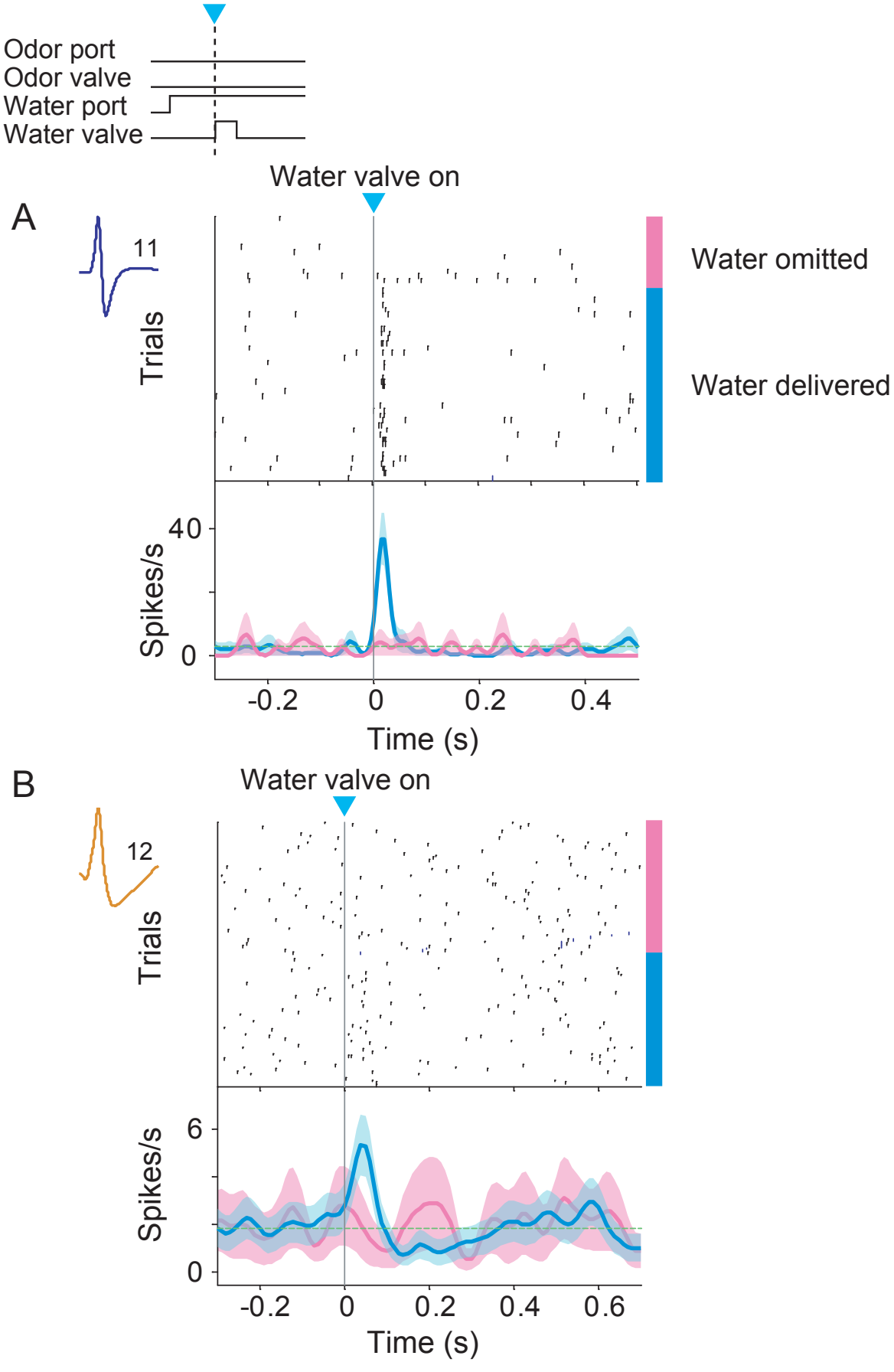

Supplementary figure - 5 (Mainen)

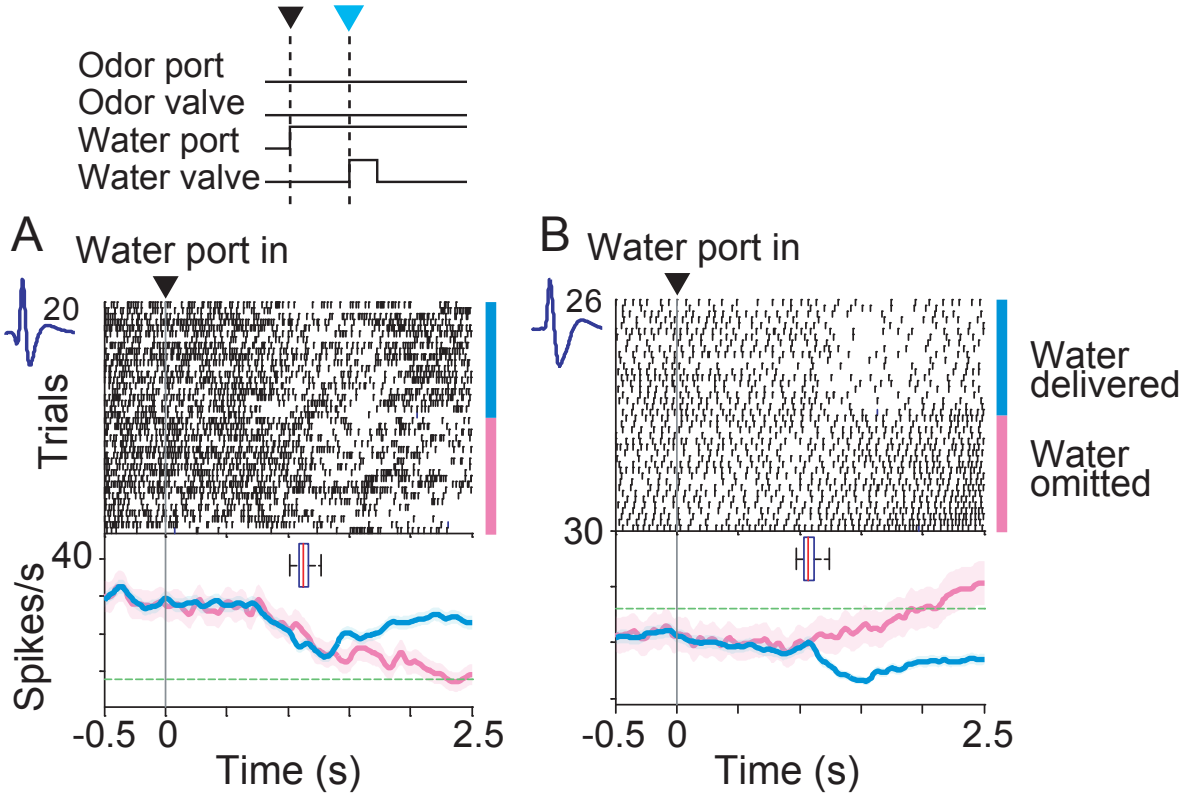

Supplementary figure - 6 (Mainen)